JCB Journal of Cell Biology

ARTICLE

PLK4-phosphorylated NEDD1 facilitates cartwheel assembly and centriole biogenesis initiations

Wangfei Chi, Gang Wang, Guangwei Xin, Qing Jiang, and Chuanmao Zhang

Centrosome duplication occurs under strict spatiotemporal regulation once per cell cycle, and it begins with cartwheel assembly and daughter centriole biogenesis at the lateral sites of the mother centrioles. However, although much of this process is understood, how centrosome duplication is initiated remains unclear. Here, we show that cartwheel assembly followed by daughter centriole biogenesis is initiated on the NEDD1-containing layer of the pericentriolar material (PCM) by the recruitment of SAS-6 to the mother centriole under the regulation of PLK4. We found that PLK4-mediated phosphorylation of NEDD1 at its S325 amino acid residue directly promotes both NEDD1 binding to SAS-6 and recruiting SAS-6 to the centrosome. Overexpression of phosphomimicking NEDD1 mutant S325E promoted cartwheel assembly and daughter centriole biogenesis initiations, whereas overexpression of nonphosphorylatable NEDD1 mutant S325A abolished the initiations. Collectively, our results demonstrate that PLK4-regulated NEDD1 facilitates initiation of the cartwheel assembly and of daughter centriole biogenesis in mammals.

Introduction

Centrosomes, the main microtubule-organizing centers, are responsible for organizing the interphase microtubule cytoskeleton and the mitotic spindle, which are crucial for both intracellular material transport and chromosome segregation during cell division in vertebrates. Centrosomal dysfunction has been frequently linked to numerous serious diseases and disorders, including cancer, dysplasia, brain developmental disorders, degeneration, and others (Bornens, 2012; Conduit et al., 2015; Nigg and Holland, 2018; Nigg and Raff, 2009). A mature centrosome is composed of a pair of centrioles surrounded by pericentriolar material (PCM). A mature centriole is a cylindrical structure with rotational symmetry made up of nine triplet microtubules with distinct species-dependent lengths, while PCM is a highly ordered hierarchical architecture with components that occupy separate spatial domains around the mother centriole (Lawo et al., 2012; Lukinavičius et al., 2013; Mennella et al., 2012). The PCM in interphase is usually small, and it adopts a concentric toroidal distribution with a varying diameter, but in mitosis, the PCM expands dramatically and hosts more components (Lee and Rhee, 2011; Lüders, 2012; Joukov et al., 2014; Fu and Zhang, 2019; Novak et al., 2016; Ramani et al., 2018).

Centrosome duplicates once per cell cycle via the generation of two daughter centrioles, each at a site on the two preexisting mother centrioles. After the two new centrioles have formed, PCM components are added to each of the new centriole pairs. Daughter centriole biogenesis initiates during early S phase with cartwheel assembly at the proximal lateral side of each mother centriole. The cartwheel consists of a central ring (hub) with nine radial spokes, followed by the assembly of a cylindrical microtubule triplet around the cartwheel (Kitagawa et al., 2011; Wang et al., 2014). SAS-6 is the key structural components that makes up the central part of the cartwheel (Keller et al., 2014; van Breugel et al., 2011), and Cep135 is another structural component that forms the distal part of the cartwheel and connects it to the microtubule triplets (Lin et al., 2013a). Also located on the cartwheel, STIL binds and assists SAS-6 in cartwheel assembly (Arquint et al., 2012; Tang et al., 2011). Additionally, generation or biogenesis of the daughter centrioles also requires multiple functions of the PCM. Both Cep192 and Cep152 are scaffold components of the PCM and essential for the recruitment of PLK4, a known master regulator of daughter centriole biogenesis, to the PCM (Kim et al., 2013; Sonnen et al., 2013). Also, both γ-tubulin and SPD-5 (known as CDK5RAP2 in humans) participate in daughter centriole biogenesis, with γ-tubulin nucleating the microtubule triplets of the centriolar cylinder, thus influencing daughter centriole assembly (Dammermann et al., 2004). Recently, pericentrin (PCNT), also a structural PCM component, was found to recruit Sas-6 for centriole assembly in *Drosophila* cells (Ito et al., 2019).

The Key Laboratory of Cell Proliferation and Differentiation of the Ministry of Education, College of Life Sciences, Peking University, Beijing, China.

Correspondence to Chuanmao Zhang: zhangcm@pku.edu.cn.

© 2020 Chi et al. This article is distributed under the terms of an Attribution–Noncommercial–Share Alike–No Mirror Sites license for the first six months after the publication date (see http://www.rupress.org/terms/). After six months it is available under a Creative Commons License (Attribution–Noncommercial–Share Alike 4.0 International license, as described at https://creativecommons.org/licenses/by-nc-sa/4.0/).

Check for updates

Downloaded from http://rupress.org/jcb/article-pdf/220/1/e202002151/1621362/jcb_202002151.pdf by guest on 09 February 2026

To duplicate the centrosomes, PLK4, a protein kinase, but not a structural component of the PCM, directly interacts with and phosphorylates STIL to facilitate formation of the STIL–SAS-6 complex (Moyer et al., 2015; Ohta et al., 2014). Using super-resolution microscopy, the PCM was saw to be periodically organized into a larger, overlapping, layered structure around the mother centrioles, along with structural components, including Cep120, Cep192, CDK5RAP2, NEDD1, TUBG1, and PCNT (Lawo et al., 2012). However, whether PCM components contribute to cartwheel assembly initiation and subsequent centriole biogenesis has not yet been elucidated, and thus, the underlying mechanism governing cartwheel assembly initiation and subsequent centriole biogenesis in mammalian cells remains poorly understood, although much progress in understanding centrosome duplication has been achieved.

In this work, we found that NEDD1 is required for both initiation of cartwheel assembly and subsequent daughter centriole biogenesis on the mother centriolar PCM by serving as a pedestal. We revealed that NEDD1 directly binds SAS-6 under the regulation of PLK4 to promote cartwheel assembly and daughter centriole biogenesis on the NEDD1-containing PCM layer. We also demonstrated that PLK4 phosphorylates NEDD1 in the PCM, at least at S325, to recruit SAS-6 to the cartwheel assembly site, thus stabilizing the SAS-6 and STIL complex for cartwheel assembly and subsequent daughter centriole biogenesis.

Results

NEDD1 facilitates cartwheel assembly initiation and stabilizes the cartwheel structure

To investigate the mechanism that governs centrosome duplication initiation, we first determined which layer of the PCM is essential for cartwheel assembly and stabilization. Since SAS-6 is the key structural component that comprises the central part of the cartwheel, we regarded SAS-6 recruitment to the proximal lateral side of the mother centriole as a criterion for cartwheel assembly initiation. Using RNAi screening, we found that while NEDD1 knockdown abolished SAS-6 recruitment to the site of the mother centriole, individual knockdown of γ-tubulin or CDK5RAP2, reportedly essential for daughter centriole biogenesis in *Caenorhabditis elegans,* had no effect on the recruitment of SAS-6 (Fig. 1, A and B; and Fig. S1 A), thus indicating that NEDD1, but not γ-tubulin or CDK5RAP2, is found upstream of SAS-6 during cartwheel assembly initiation. Furthermore, when we investigated the recruitment of other centrosome proteins related to centrosome duplication in cells with RNAi-mediated knockdown, we found that the recruitment of STIL to the lateral site of the mother centriole was also abolished in NEDD1-knockdown cells, but not in γ-tubulin– or CDK5RAP2-knockdown cells (Fig. 1, C and D; and Fig. S1, A–E). However, centrosomal recruitment of PLK4, Cep152, and Cep192 is not affected by NEDD1 knockdown (Fig. 1, C and D), suggesting that NEDD1 acts directly on cartwheel assembly initiation rather than indirectly by affecting PLK4. To further prove that NEDD1 is required for cartwheel assembly initiation, a coimmunoprecipitation (coIP) assay revealed that the interaction between SAS-6 and STIL was attenuated in NEDD1-knockdown, but not in γ-tubulin-knockdown, cells without changes in SAS-6, STIL, PLK4, and γ-tubulin protein levels, all of which are important for centriole biogenesis (Fig. 1 E and Fig. S1 F). In addition, when we purified Strep-NEDD1 and GFP-SAS-6-Strep from HEK293F cells and then performed a GFP pull-down assay by incubating with Myc-STIL–expressing cell lysate, we found that adding NEDD1 enhances the interaction between SAS-6 and STIL in vitro (Fig. S1 G). These findings suggest that NEDD1 knockdown impairs the centrosomal localization of SAS-6 and STIL, thus destroying cartwheel structure stability. Taken together, these results demonstrate that NEDD1 in the PCM is required for cartwheel assembly and structural stability.

Next, using structured illumination microscopy (SIM), we investigated the precise localization of the related proteins required for cartwheel assembly and centriole biogenesis. We identified that centrosomal NEDD1 adopted a ring-like architecture around the mother centriole toward its proximal end in the G1 phase and gradually extended toward the daughter centriole as the cell cycle progressed (Fig. S1 H). Since Cep192 is important for recruiting NEDD1 to the centrosomes (Zhu et al., 2008) and the suggested roles for Cep192 in centriole duplication are contradictory (Gomez-Ferreria et al., 2007; Kim et al., 2013; Sonnen et al., 2013), we decided to further investigate how NEDD1 is recruited to the PCM. We found that Cep192 depletion significantly decreased NEDD1, but not PCNT, on the centrosomes and abolished centrosomal SAS-6. Additionally, PCNT depletion also reduced the signal intensity of NEDD1 and SAS-6 on the centrosomes (Fig. S2, A–D). When Cep192 and PCNT were both depleted, centrosomal NEDD1 almost completely vanished (Fig. S2, E and F). These results demonstrate that both Cep192 and PCNT are upstream of NEDD1 and function together to recruit NEDD1 to the PCM. Also, unlike *Drosophila* PCNT, human PCNT may indirectly affect the recruitment of SAS-6 via NEDD1.

We explored the spatiotemporal relationships between NEDD1 and cartwheel proteins to further determine whether the cartwheel assembly is initiated on the NEDD1-containing layer. Since endogenous cartwheel proteins SAS-6 and STIL are restricted to a single site at each of the two mother centrioles, where they initiate daughter centriole biogenesis (Fig. 1, A and C), and PLK4 overexpression induces artificial centriole amplification (Kleylein-Sohn et al., 2007), we also expressed Myc-tagged PLK4 and examined localization of the related proteins. We found that NEDD1 colocalized with Myc-PLK4 in a small ring-like structure, while γ-tubulin was assembled into a ring larger than the NEDD1 ring, and NEDD1 was partially colocalized inside that ring (Fig. 1, F and G). Interestingly, SAS-6 and STIL also assembled into larger rings around the NEDD1 ring, and the inner sites of the SAS-6/STIL rings colocalized with NEDD1 (Fig. 1, F and G). Based on these findings, we drew a model to show the spatial relationship among the related proteins (Fig. 1 H). Taken together, these results indicate that cartwheel assembly initiates on the NEDD1 layer, which is locally recruited by Cep192 and PCNT and is essential for the recruitment of the cartwheel proteins SAS-6 and STIL.

NEDD1 is essential for daughter centriole biogenesis

Knowing NEDD1 is required for cartwheel assembly initiation, we then investigated whether NEDD1 is also essential

Downloaded from http://rupress.org/jcb/article-pdf/220/1/e202002151/1621362/jcb_202002151.pdf by guest on 09 February 2026

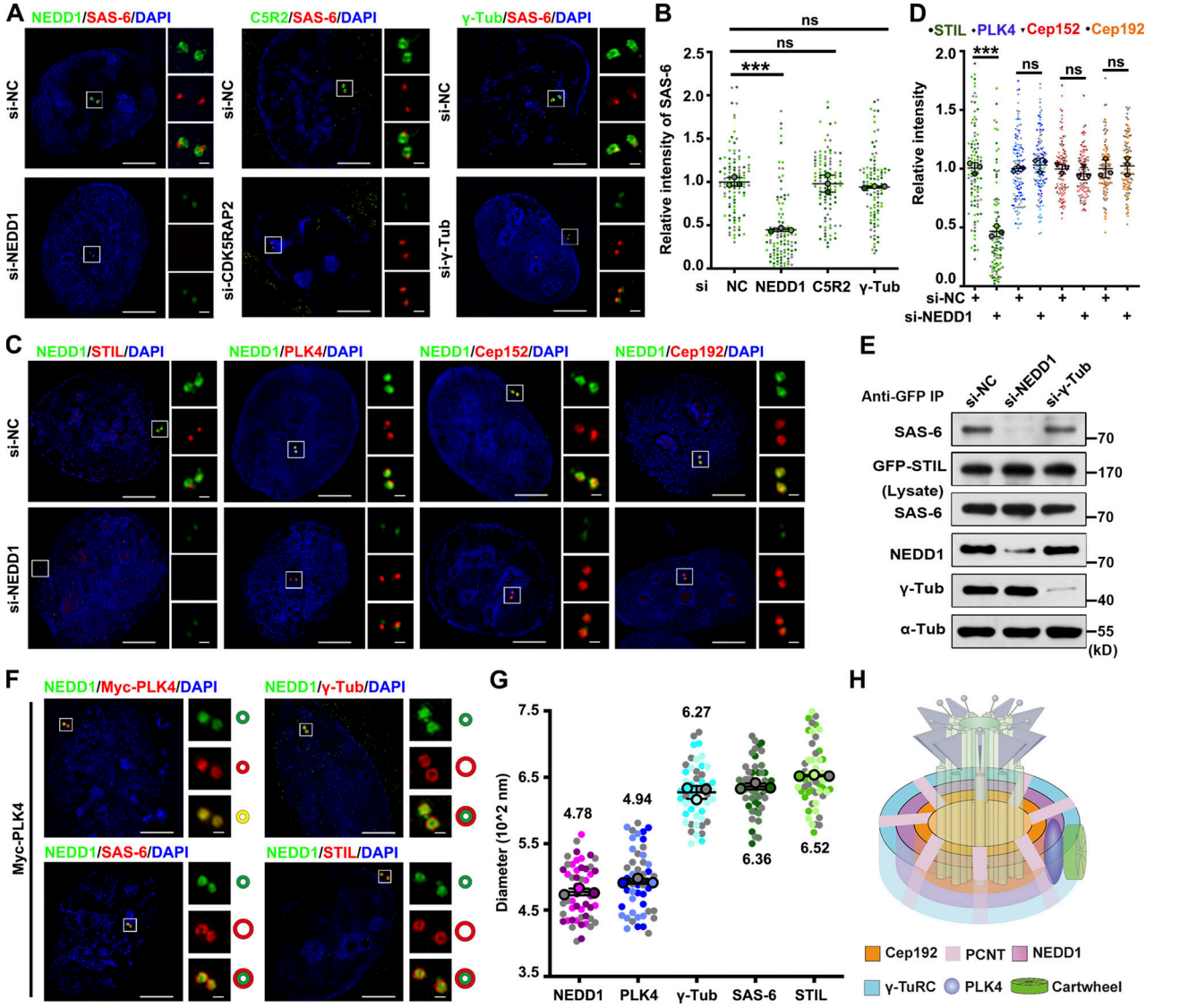

Figure 1. **NEDD1 facilitates cartwheel assembly initiation and stabilizes the cartwheel structure. (A)** U2OS cells treated with siRNA against NEDD1, CDK5RAP2, or γ-tubulin were coimmunostained with antibodies against NEDD1, CDK5RAP2, or γ-tubulin and SAS-6. C5R2, CDK5RAP2. DNA was stained with DAPI. Scale bars, 5 µm (large images) or 0.5 µm (inset images). **(B)** Comparisons of relative fluorescence intensity of SAS-6 in A. Three independent replicates of >30 cells per replicate were quantified. **(C)** U2OS cells treated with siRNA against control or NEDD1 were coimmunostained with antibodies against NEDD1 and STIL, PLK4, Cep152, or Cep192. DNA was stained with DAPI. Scale bars, 5 µm (large images) or 0.5 µm (inset images). **(D)** Comparisons of the relative fluorescence intensity of related proteins in C. Three independent replicates of >30 cells per replicate were quantified. **(E)** HEK293T cells were transfected with GFP-STIL and treated with control, NEDD1, or γ-tubulin siRNA. Total cell extracts were immunoprecipitated with GFP-Trap beads and probed with antibodies against SAS-6, GFP, NEDD1, γ-tubulin, and α-tubulin. **(F)** Immunofluorescence of NEDD1 and γ-tubulin, SAS-6, STIL, or Myc in U2OS cells transfected with Myc-PLK4. The stained proteins' centrosomal features are shown in the cartoons below each image. DNA was stained with DAPI. Scale bars, 5 µm (large images) or 0.5 µm (inset images). **(G)** Quantification of outer toroid/ring diameters (with means) of the indicated cartwheel or PCM proteins in U2OS cells at interphase. Three independent replicates of >15 cells per replicate were quantified. **(H)** Organizational features of the interphase PCM components. Error bars in B, D, and G indicate mean ± SD. ***, P < 0.001; ns, no significant difference (two-tailed *t* test). NC, negative control; Tub, tubulin.

for daughter centriole biogenesis. Through an RNAi knockdown experiment followed by immunofluorescence staining for Centrin1, we observed that >80% of the NEDD1-knockdown cells contained fewer than four discernable centrioles (Fig. S3, A and B), suggesting severe centriole biogenesis defects in NEDD1-knockdown cells. Next, we treated U2OS cells with hydroxyurea (HU), a chemical that blocks the cell cycle at S phase without influencing centrosome duplication, to induce centrosome overduplication and found that HU treatment could not induce endogenous centrosome overduplication in NEDD1-knockdown cells (Fig. S3, C and D). Since overexpression of PLK4 is sufficient to induce centrosome amplification (Kleylein-Sohn et al., 2007), we also expressed PLK4-GFP in U2OS cells to induce centrosome amplification, and while ~60% of PLK4-GFP–positive cells showed an excessive assembly of centrioles into rosette-like structures, PLK4-GFP overexpression was still unable to induce centrosome amplification in NEDD1-knockdown cells (Fig. 2, A and B). Altogether,

Downloaded from http://rupress.org/jcb/article-pdf/220/1/e202002151/1621362/jcb_202002151.pdf by guest on 09 February 2026

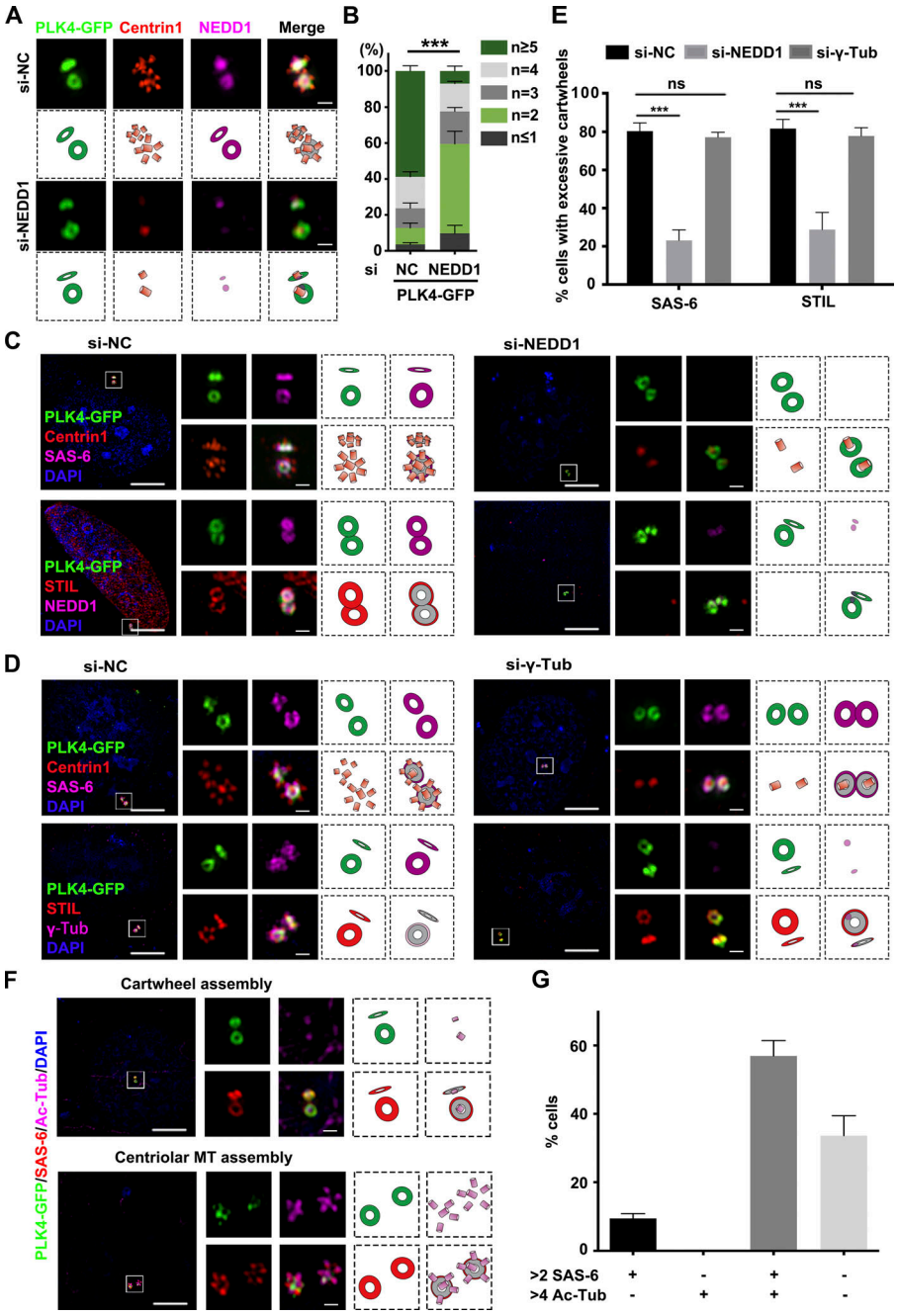

Figure 2. **NEDD1 is essential for daughter centriole biogenesis. (A)** U2OS cells transfected with PLK4-GFP for 20 h after treatment with control or NEDD1 siRNA were stained with antibodies against Centrin1 and SAS-6. DNA was stained with DAPI. The stained proteins' centrosomal features are shown in the cartoons below each image. Scale bars, 0.5 µm. **(B)** Percentages of the cells with different numbers of centrioles and comparisons of those cells with more than four centrioles in each treatment in A. Three independent replicates of >100 cells per replicate were quantified. **(C and D)** U2OS cells were transfected with PLK4-GFP for 20 h after treatment with control, NEDD1 siRNA (C), or γ-tubulin siRNA (D) and then stained with antibodies against Centrin1 and SAS-6 or against STIL and either NEDD1 (C) or γ-tubulin (D). DNA was stained with DAPI. The stained proteins' centrosomal features are shown in the cartoons to the right of each image. Scale bars, 5 µm (large images) or 0.5 µm (inset images). **(E)** Comparisons of cells with more than two SAS-6 or STIL dots. Three independent replicates of >100 cells per replicate were quantified. **(F)** U2OS cells transfected with PLK4-GFP were coimmunostained with antibodies against SAS-6 and acetylated tubulin (Ac-Tub). DNA was stained with DAPI. The stained proteins' centrosomal features are shown in the cartoons to the right of each image. Scale bars, 5 µm (large images) or 0.5 µm (inset images). **(G)** Comparisons of the percentages of cells with the given number of SAS-6 dots and acetylated tubulin dots after PLK4 overexpression. Three independent replicates of >100 cells per replicate were quantified. Error bars in B, E, and G indicate mean ± SD. ***, $P < 0.001$; ns, no significant difference (two-tailed *t* test). NC, negative control; Tub, tubulin.

these results demonstrate that NEDD1 is essential for daughter centriole biogenesis.

To determine in which step in daughter centriole biogenesis NEDD1 functions, we examined cartwheel assembly and daughter centriole biogenesis in PLK4-GFP–overexpressing cells with NEDD1 knocked down. The results showed that in control knockdown cells, both PLK4-GFP and NEDD1 were colocalized in a ring-like structure, and cartwheel assembly occurred around that ring, as indicated by SAS-6- and STIL-positive staining. Furthermore, using Centrin1-positive staining we observed excess biogenesis of daughter centrioles in a rosette-like pattern (Fig. 2, C and E). However, NEDD1 knockdown did not affect PLK4-GFP ring-like structure formation but instead abolished both cartwheel assembly and centriole biogenesis around the mother centriole (Fig. 2, C and E), indicating that both cartwheel assembly and daughter centriole biogenesis require NEDD1. To distinguish whether cartwheel assembly and daughter centriole biogenesis are sequential or simultaneous processes, we knocked down γ-tubulin and confirmed that daughter centriole biogenesis was blocked in these cells (Fig. S3, E and F), thus suggesting that the blockade of daughter centriole biogenesis does not affect the recruitment of SAS-6 and STIL for cartwheel assembly. To confirm this, we also examined both cartwheel assembly and daughter centriole biogenesis after γ-tubulin knockdown in PLK4-GFP–overexpressing cells and found that the PLK4-GFP ring and SAS-6/STIL cartwheel remained in γ-tubulin–knockdown cells, while daughter centriole biogenesis was completely abolished (Fig. 2, D and E).

Downloaded from http://rupress.org/jcb/article-pdf/220/1/e202002151/1621362/jcb_202002151.pdf by guest on 09 February 2026

These results indicate that cartwheel assembly and daughter centriole biogenesis are sequential processes and that NEDD1 can recruit SAS-6 and STIL for cartwheel formation independent of γ-tubulin. Given that NEDD1 is required for the recruitment of γ-tubulin to the centrosomes for mitotic spindle assembly (Zhang et al., 2009), we investigated whether depletion of γ-tubulin or of NEDD1 affects centriolar microtubule nucleation during daughter centriole biogenesis and discovered that depletion of either NEDD1 or γ-tubulin abolished microtubule nucleation of the daughter centrioles (Fig. S3, G and H). Consistently, when PLK4-GFP was overexpressed, the number of cells with excessive cartwheels was greater than that with excessive daughter centrioles (Fig. 2, F and G), indicating that cartwheel assembly occurs earlier than centriolar microtubule nucleation. Collectively, these results demonstrate that NEDD1 is required for initiating sequential cartwheel assembly and daughter centriole biogenesis.

NEDD1 facilitates initiation of the cartwheel assembly by directly recruiting SAS-6

Next, we investigated how NEDD1 facilitates cartwheel assembly initiation. By using coIP, protein–protein interaction assays, and immunofluorescence labeling, we discovered that NEDD1 interacted strongly with SAS-6, regardless of whether it was endogenously expressed or exogenously transfected as a tagged protein, but only weakly with STIL (Fig. 3, A–C; and Fig. S4, A and B). Therefore, we speculated that NEDD1 facilitates cartwheel assembly initiation by recruiting SAS-6. To understand why NEDD1 knockdown also caused removal of STIL from the centrosome, we used RNAi to explore how SAS-6 and STIL exist together in their centrosomal localization. We found that, consistent with a previous report that SAS-6 and STIL are mutually dependent for their centrosomal localization (Tang et al., 2011), STIL knockdown indeed reduced the intensity of SAS-6 on the centrosome, but knocking down SAS-6 affected the centrosomal localization of STIL even more severely (Fig. S4, C–G). These results indicated that NEDD1 facilitates cartwheel assembly initiation directly by recruiting SAS-6, which then binds STIL for cartwheel assembly. We also believe that NEDD1 depletion impairs STIL due to removal of SAS-6 from the centrosome and detriment of the stabilized cartwheel structure. Next, we used reciprocal coIP of HEK293T cells coexpressed either with truncated GFP-tagged SAS-6 proteins with Myc-tagged NEDD1 or with truncated GFP-tagged NEDD1 proteins to determine the regions of both SAS-6 and NEDD1 that mediate their interaction. We observed that the coiled-coil domain and C-terminal truncated SAS-6 proteins interacted with the N-terminal truncated NEDD1 protein containing WD40 repeats, thus further indicating that NEDD1 and SAS-6 engage in functional interplay on centrosomes (Fig. 3, D–F). coIP of HEK293T cells transfected with GFP-NEDD1 and synchronized to the G1/S transition or the S, G2, or M phase, showed that NEDD1 and SAS-6 interaction occurs mainly in the S phase (Fig. 3 G), a finding consistent with the timing of NEDD1-mediated initiation of both cartwheel assembly and daughter centriole biogenesis in the S phase. Next, we performed SAS-6– and STIL-knockdown experiments with coimmunostained NEDD1 and found no obvious changes in both the localization patterns and the intensity of NEDD1 on the centrosome in both SAS-6– or STIL-knockdown cells (Fig. 3, H and I), confirming that NEDD1 is situated upstream of SAS-6 during cartwheel assembly. Collectively, these results demonstrate that NEDD1 directly interacts with and recruits SAS-6 to the PCM in early S phase to facilitate the initiation of both cartwheel assembly and subsequent daughter centriole biogenesis.

NEDD1 is phosphorylated by PLK4 at six amino acid residues

Since NEDD1, as a PCM component, adopts a toroidal distribution around the mother centriole and timely facilitates cartwheel assembly initiation at only one site on that centriole, we wondered how its functions are regulated. Since we observed that NEDD1 is highly colocalized with overexpressed PLK4 (Fig. 1 F), we decided to further investigate their relationship. Through coIP, we found that NEDD1 and PLK4 also interacted in vivo, regardless of whether they were endogenously expressed or exogenously transfected (Figs. 3 A, 4 A, and S4 H). Since PLK4 had been reported to phosphorylate several proteins involved in the centrosome cycle (Bahtz et al., 2012; Lee et al., 2017; Xu et al., 2017), we wondered whether NEDD1 is a novel substrate for PLK4. Through a GST pull-down assay using purified proteins, we confirmed that PLK4 and NEDD1 interacted in vitro (Fig. 4 B and Fig. S4 I). To determine which PLK4 and NEDD1 regions mediate their interaction, we coexpressed truncated GFP-tagged NEDD1 proteins and Myc-tagged PLK4 or truncated GFP-tagged PLK4 proteins and performed coIP experiments. We found that the NEDD1 N-terminus and the PB1 and PB2 domains of PLK4 mediate their interaction (Fig. 4, C–E). We also showed that NEDD1 obviously interacted with PLK4 at the G1/S transition, which obviously occurred before the interaction of NEDD1 with SAS-6 (Fig. 3 G). By inhibiting PLK4 kinase activity with centrinone B, we found that the interaction between NEDD1 and PLK4 was not dependent on PLK4 kinase activity (Fig. S4 J). Taken together, these data demonstrate that NEDD1 interacts with the PB1 and PB2 domains of PLK4 via its N-terminus during the G1/S transition.

Next, using an in vitro kinase assay, we further investigated whether NEDD1 is phosphorylated by PLK4. First, we purified Strep-NEDD1 from HEK293F cells and then dephosphorylated the protein using λ-PPase. The resulting protein then underwent detection with mass spectrometry (MS) to confirm that it was not phosphorylated. Then, after incubating the unphosphorylated Strep-NEDD1 with purified PLK4, we detected the phosphorylation sites in NEDD1 with a second round of MS (Fig. 4 F). The results showed that six amino acid residues in NEDD1 were phosphorylated by PLK4 (Fig. S5 A). Among those sites, four (T23, T303, S325, and S338) are located in the N-terminus, and the remaining two (S404 and S568) are located in the C-terminus (Fig. 4 F). Next, we mutated those six amino acid residues into alanine residues (6A) and expressed Strep-tagged NEDD1 WT and mutant proteins in HEK293F cells. Those proteins were then purified and incubated with purified PLK4 in the presence of [γ-^{32}P]-ATP for an in vitro kinase assay. The results revealed that NEDD1 WT was phosphorylated by PLK4, while the NEDD1 6A mutant suffered severely impaired

Downloaded from http://rupress.org/jcb/article-pdf/220/1/e202002151/1621362/jcb_202002151.pdf by guest on 09 February 2026

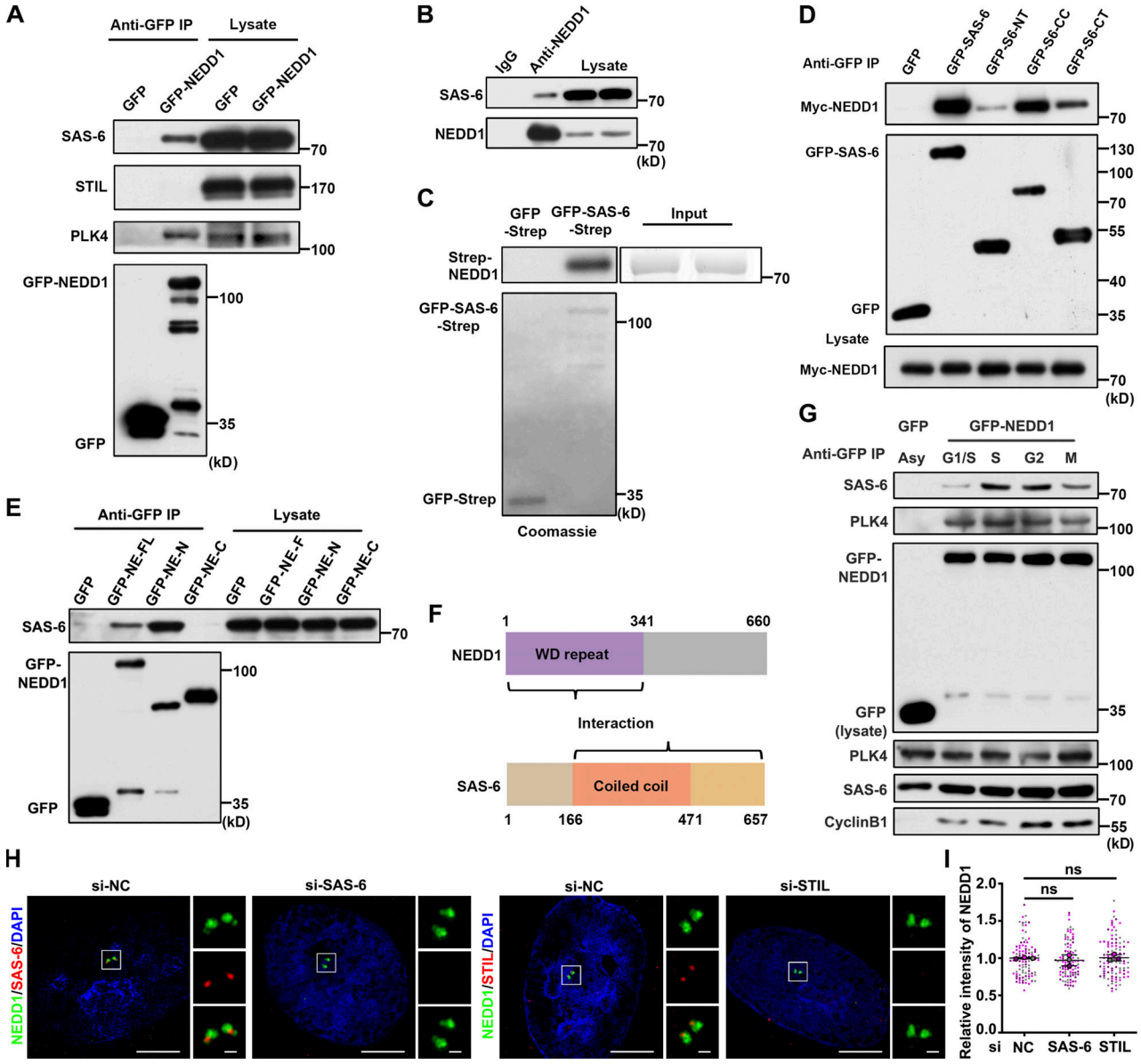

Figure 3. **NEDD1 facilitates initiation of cartwheel formation by directly recruiting SAS-6. (A)** Total extracts of HEK293T cells expressing GFP-NEDD1 were immunoprecipitated with GFP-Trap beads and probed with antibodies against SAS-6, STIL, and PLK4. **(B)** Total extracts of HEK293T cells were immunoprecipitated with anti-NEDD1 antibody and probed with antibodies against SAS-6 and NEDD1. **(C)** In vitro SAS-6 and NEDD1 binding assay. GFP-Trap beads coupled with purified GFP-Strep or GFP-SAS-6-Strep were incubated with purified Strep-NEDD1 and analyzed using anti-NEDD1 antibody. The indicated protein loads are shown by Coomassie blue staining. **(D)** Total extracts of HEK293T cells cotransfected with Myc-NEDD1 and full-length or truncated GFP–SAS-6 proteins were immunoprecipitated with GFP-Trap beads and probed with antibodies against Myc and GFP. **(E)** Total extracts of HEK293T cells transfected with full-length or truncated GFP-NEDD1 were immunoprecipitated with GFP-Trap beads and probed with antibodies against SAS-6 and GFP. **(F)** Schematic of the interactions between NEDD1 and SAS-6. **(G)** HEK293T cells transfected with GFP-NEDD1 and synchronized at the G1/S transition were released into fresh medium for the indicated phases. The total cellular extracts were then immunoprecipitated with GFP-Trap beads and probed with antibodies against SAS-6, PLK4, and GFP. Cyclin B1 was used as a marker for the M phase. **(H)** U2OS cells treated with siRNA against SAS-6 or STIL were coimmunostained with antibodies against NEDD1 and SAS-6 or NEDD1 and STIL. DNA was stained with DAPI. Scale bars, 5 µm (large images) or 0.5 µm (inset images). **(I)** Comparisons of the relative fluorescence intensities of NEDD1 in H. Three independent replicates of >30 cells per replicate were quantified. Error bars indicate mean ± SD. ns, no significant difference (two-tailed *t* test). NC, negative control; WD repeat, Tryptophan-Aspartic acid repeat.

phosphorylation (Fig. 4, G and H). Through immunofluorescence labeling, we observed that the 6A mutant was still normally localized to the centrosomes (Fig. 4 I), suggesting that multisite phosphorylation is not essential for NEDD1 to localize to the centrosomes. Consistently, through coIP, we discovered that the interaction between NEDD1 WT and Cep192, which recruits NEDD1 to the centrosomes, was not significantly different from the interaction between the 6A mutant and Cep192 (Fig. 4 J). Taken together, these results demonstrate that PLK4 binds NEDD1 and phosphorylates NEDD1 at multiple sites and that the phosphorylation of NEDD1 by PLK4 does not affect its centrosomal localization.

Downloaded from http://rupress.org/jcb/article-pdf/220/1/e202002151/1621362/jcb_202002151.pdf by guest on 09 February 2026

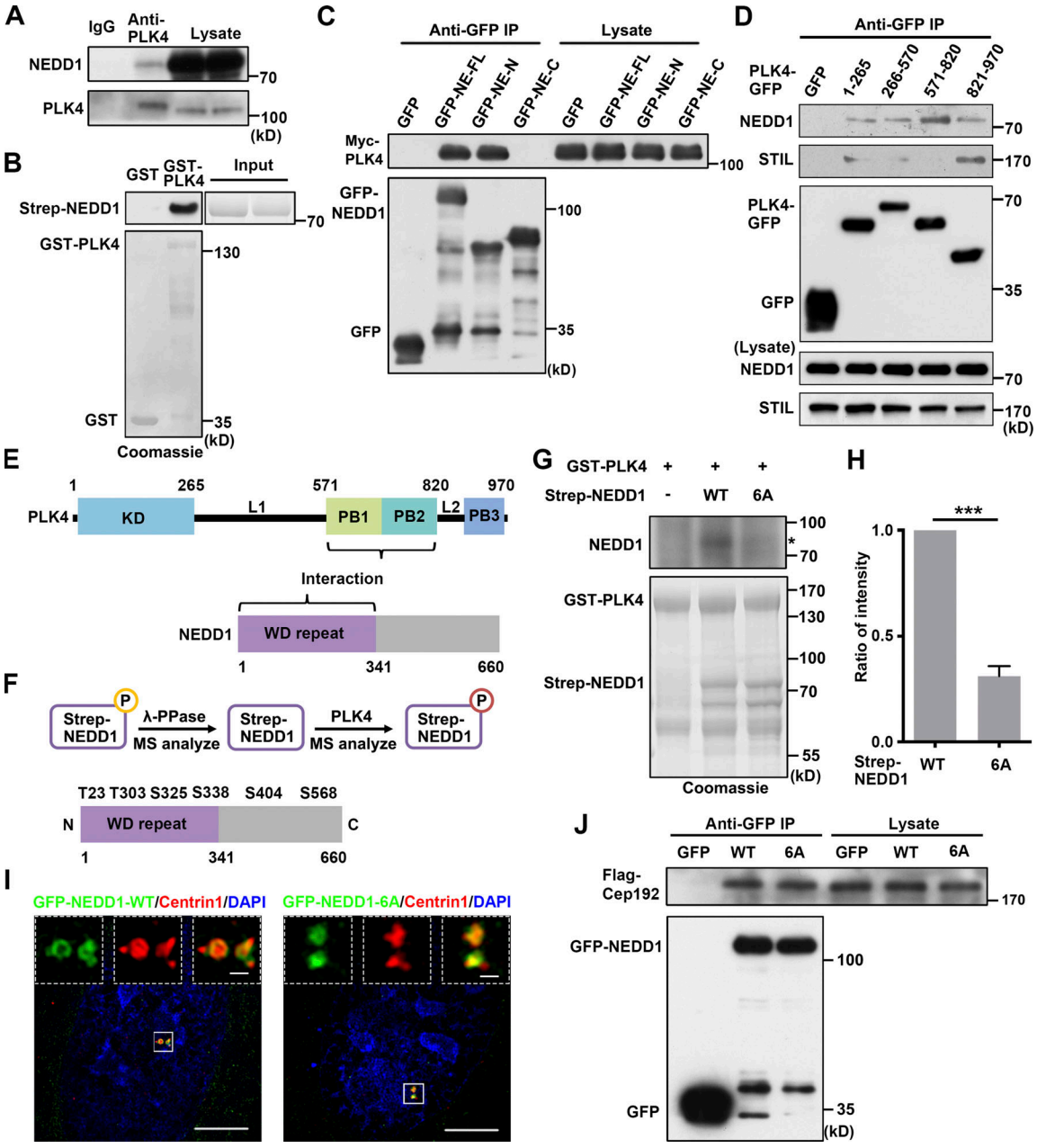

Figure 4. **PLK4 phosphorylates NEDD1 at six sites. (A)** Total extracts of HEK293T cells were immunoprecipitated with anti-PLK4 antibody and probed with antibodies against NEDD1 and PLK4. **(B)** In vitro PLK4 and NEDD1 binding assay. Sepharose beads coupled with purified GST or GST-PLK4 were incubated with purified Strep-NEDD1 and analyzed with anti-NEDD1 antibody. The indicated protein loads are shown by Coomassie blue staining. **(C)** Total extracts of HEK293T cells cotransfected with Myc-PLK4 and full-length or truncated GFP-NEDD1 were immunoprecipitated with GFP-Trap beads and probed with antibodies against Myc and GFP. FL, full-length; N, N-terminus; C, C-terminus. **(D)** Total extracts of HEK293T cells transfected with truncated PLK4-GFP immunoprecipitated with GFP-Trap beads and probed with antibodies against GFP and NEDD1 and STIL. **(E)** Schematic of the interactions between PLK4 and NEDD1 domains. **(F)** Strep-NEDD1 was dephosphorylated by λ-PPase and incubated with PLK4 before MS analysis (top diagram) revealed that PLK4 phosphorylates NEDD1 at six sites in vitro (bottom diagram). **(G)** In vitro kinase assay showing NEDD1 phosphorylation by PLK4. Purified GST-PLK4 was incubated with purified Strep-NEDD1 or NEDD1 targeted amino acid residues mutated into alanine residues (6A) in the presence of [γ-^{32}P]-ATP, followed by autoradiography. Coomassie blue staining shows the indicated protein loads. *, phosphorylated NEDD1. **(H)** Comparisons for WT and 6A mutant NEDD1 phosphorylation in G from three independent experiments. The relative intensity of the phosphorylation signal of each protein was normalized to its protein level by ImageJ. The phosphorylation signal intensity of WT NEDD1 was arbitrarily set as 1.0. Error bars indicate mean ± SD. ***, $P < 0.001$ (two-tailed *t* test). **(I)** Immunofluorescence of Centrin1 in U2OS cells transfected with GFP-tagged WT NEDD1 or GFP-tagged 6A mutant NEDD1. DNA was stained with DAPI. Scale bars, 5 µm (large images) or 0.5 µm (inset images). **(J)** Total extracts of HEK293T cells cotransfected with GFP-tagged WT or 6A mutant NEDD1 and Flag-Cep192 were immunoprecipitated with GFP-Trap beads and probed with antibodies against Flag and GFP. KD, kinase domain; PB, polo box; WD repeat, Tryptophan-Aspartic acid repeat.

Downloaded from http://rupress.org/jcb/article-pdf/220/1/e202002151/1621362/jcb_202002151.pdf by guest on 09 February 2026

Phosphorylation of NEDD1 at S325 by PLK4 regulates its interaction with SAS-6

To explore the functions of PLK4-phosphorylated NEDD1, we treated U2OS cells with centrinone B for 24 h and immunostained the cells with related antibodies. The results showed that, as expected, NEDD1 was still localized on the centrosomes, but interestingly, SAS-6 was absent from its usual site for cartwheel assembly and daughter centriole biogenesis (Fig. 5 A). Using coIP analysis with SAS-6 antibody, we detected the interaction between NEDD1 and SAS-6 was significantly attenuated by treatment with centrinone B (Fig. 5 B), thus indicating that NEDD1 phosphorylation by PLK4 is required for its binding and recruitment of SAS-6 to the centrosomes. We further investigated whether all six of the identified phosphorylation sites contribute to the regulation of NEDD1 and SAS-6 binding. coIP analysis revealed that the interaction between SAS-6 and the NEDD1 6A mutant was much weaker than that between SAS-6 and NEDD1 WT (Fig. 5 C). With an MS assay using Strep-NEDD1 as bait, we found that the interaction between PLK4-phosphorylated NEDD1 and SAS-6 was stronger than that of unphosphorylated NEDD1 and SAS-6 (Fig. S5 B). Next, we constructed NEDD1 mutants with a single-site mutation to simulate an unphosphorylated state and detect their interactions with SAS-6. The results showed that the binding of Nedd1 S325A with SAS-6 was much weaker than that of NEDD1 WT or the other NEDD1 mutants with SAS-6 (Fig. 5 D and Fig. S5 C). Then, purified PLK4 was incubated with either NEDD1 WT or the S325A mutant protein in the presence of [γ-^{32}P]-ATP for an in vitro kinase assay, and it was shown that the NEDD1 S325A mutant had significantly attenuated its phosphorylation by PLK4 (Fig. S5 D). By comparing of NEDD1 amino acid sequences in different species, we found that NEDD1 S325 is conserved among mammals (Fig. 5 E), thus pointing out the evolutionary and functional importance of this protein.

Next, through individually expressing Myc-tagged NEDD1 WT and S325A mutant proteins in NEDD1-depleted cells, we investigated their ability in rescuing defects in SAS-6 recruitment to centrosomes and cartwheel assembly caused by NEDD1 knockdown. We found that while the majority of endogenous NEDD1-knockdown cells expressing Myc-tagged NEDD1 WT showed normal SAS-6 localization to cartwheel assembly sites, most of the cells expressing Myc-tagged NEDD1 S325A failed to rescue the SAS-6 disappearance phenotype (Fig. 5, F and G), indicating that this mutant could not efficiently recruit SAS-6 to the specific sites for initiating the cartwheel assembly. As expected, the results also showed that, unlike cells expressing Myc-tagged NEDD1 WT, >60% of cells expressing Myc-tagged NEDD1 S325A did not rescue the centriole biogenesis defect caused by endogenous NEDD1 depletion (Fig. 5, H and I). Interestingly, we found that the interaction between γ-tubulin and either NEDD1 6A or S325A was stronger than that between γ-tubulin and NEDD1 WT (Fig. 5, C and D). Also, the interaction between PLK4-phosphorylated NEDD1 and other γ-TuRC (γ-tubulin ring complex) components was weaker than that between unphosphorylated NEDD1 and other γ-TuRC components (Fig. 5 J and Fig. S5 B). These results suggest that phosphorylation of NEDD1 by PLK4 is critical for NEDD1 to switch its binding target from γ-TuRC to SAS-6 to facilitate cartwheel assembly initiation. Recent research has revealed that an autonomous PLK4 oscillation at the base of the growing centriole initiates and executes centriole biogenesis in fly embryos, and while S phase progresses, the centriolar PLK4 level grows to a critical concentration that triggers its destruction until its concentration is too low to support Sas-6 and Ana2 recruitment for cartwheel growth (Aydogan et al., 2020; Aydogan et al., 2018). In addition, another study showed that reduced PLK4 activity relieves the SCF–FBXW5 complex activity to degrade centriolar SAS-6 to restrict centrosome reduplication (Puklowski et al., 2011). Accordingly, we suspected that active PLK4 phosphorylates NEDD1, unbinding it from PCM γ-TuRC and allowing it to bind and recruit SAS-6 to the proximal sides of the mother centrioles for cartwheel assembly initiation. Then, along with impaired PLK4 kinase activity, more dephosphorylated NEDD1 recruits more γ-TuRC to these sites for the initiation of daughter centriole assembly.

When we investigated the effects of S325A mutant NEDD1 on centrosome duplication with PLK4 overexpression in endogenous NEDD1-knockdown cells, we found that while most of the NEDD1-knockdown cells coexpressing Myc-tagged NEDD1 WT with PLK4-GFP showed excessive cartwheel and centriole assembly, most of the cells coexpressing Myc-tagged NEDD1 S325A with PLK4-GFP showed no cartwheel assembly and daughter centriole biogenesis (Fig. 6, A–D). This indicated that NEDD1 S325A could not support cartwheel and centriole assembly initiation and execution, even with active PLK4 present. Altogether, these results demonstrate that phosphorylation of NEDD1 by PLK4, at least at S325, promotes NEDD1 binding with SAS-6, an essential step in the initiation of both cartwheel assembly and subsequent daughter centriole biogenesis.

S325-phosphorylated NEDD1 directly recruits SAS-6 for cartwheel assembly

Since NEDD1 adopts a toroidal distribution around the mother centriole, SAS-6 is recruited to a specific site where PLK4 is localized, and overexpressed PLK4 also adopts a toroidal distribution that overlaps the NEDD1 ring and induces both the assembly of multiple cartwheels and daughter centriole biogenesis, we suspected that PLK4-phosphorylated NEDD1 facilitates the cartwheel assembly initiation by recruiting SAS-6 to the proximal sites of the mother centriole and the subsequent dephosphorylation of NEDD1 initiates the daughter centriole biogenesis by recruiting γ-TuRC to those sites. To verify this hypothesis, we constructed a phosphomimicking NEDD1 S325E mutant and expressed it in HEK293T cells. Using coIP, we found that, in contrast to the weak interaction between the NEDD1 S325A mutant and SAS-6, the interaction between NEDD1-S325E and SAS-6 was slightly stronger than that between NEDD1 WT and SAS-6 (Fig. 7 A). We further investigated the localization of both S325E and S325A mutant proteins in U2OS cells. Similar to the NEDD1 WT protein, both mutants also located to the centrosomes. Interestingly, while cells transfected with NEDD1 WT or S325A mutant showed normal levels of SAS-6, which formed dot-like structures attached to the mother centriole during the S phase, NEDD1 S325E recruited much more SAS-6 to the lateral

Downloaded from http://rupress.org/jcb/article-pdf/220/1/e202002151/1621362/jcb_202002151.pdf by guest on 09 February 2026

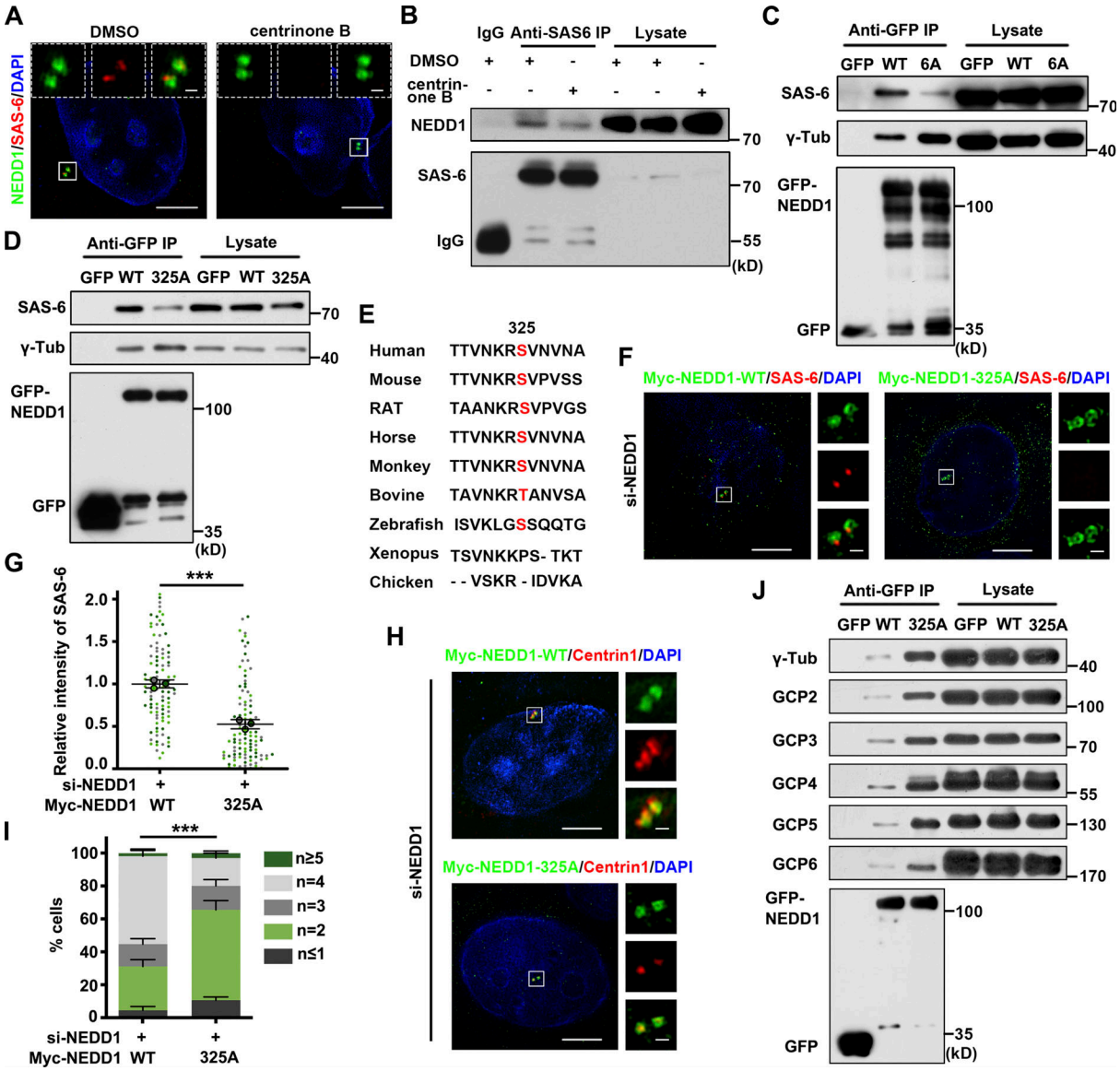

Figure 5. **PLK4 phosphorylation of NEDD1 regulates its interaction with SAS-6 for cartwheel assembly. (A)** U2OS cells were treated with either DMSO or 500 nM centrinone B for 24 h and coimmunostained with antibodies against NEDD1 and SAS-6. DNA was stained with DAPI. Scale bars, 5 µm (large images) or 0.5 µm (inset images). **(B)** Total extracts of HEK293T cells treated with DMSO or 500 nM centrinone B for 24 h were immunoprecipitated with anti–SAS-6 antibody and probed with antibodies against SAS-6 and NEDD1. **(C)** Total extracts of HEK293T cells transfected with GFP-tagged WT or 6A mutant NEDD1 were immunoprecipitated with GFP-Trap beads and probed with antibodies against SAS-6, γ-tubulin, and GFP. **(D)** Total extracts of HEK293T cells transfected with GFP-tagged WT or S325A mutant NEDD1 were immunoprecipitated with GFP-Trap beads and probed with antibodies against SAS-6, γ-tubulin, and GFP. **(E)** Partial protein sequences of NEDD1 in human, mouse, rat, horse, monkey, bovine, zebrafish, xenopus, and chicken. **(F)** U2OS cells were cotransfected with endogenous NEDD1 siRNA and Myc-tagged siRNA-resistant WT or S325A mutant NEDD1 and immunostained with anti-SAS-6 antibody. DNA was stained with DAPI. Scale bars, 5 µm (large images) or 0.5 µm (inset images). **(G)** Comparisons of the relative fluorescence intensity of SAS-6 in (F). Three independent replicates of >30 cells per replicate were quantified. **(H)** U2OS cells were cotransfected with endogenous NEDD1 siRNA and Myc-tagged siRNA-resistant WT or S325A mutant NEDD1 and coimmunostained with antibodies against Myc and Centrin1. DNA was stained with DAPI. Scale bars, 5 µm (large images) or 0.5 µm (inset images). **(I)** Percentages of the cells with different numbers of centrioles and comparisons of those cells with fewer than four centrioles in each treatment in H. Three independent replicates of >100 cells per replicate were quantified. **(J)** Total extracts of HEK293T cells transfected with GFP-tagged WT or S325A mutant NEDD1 were immunoprecipitated with GFP-Trap beads and probed with antibodies against γ-tubulin, GCP2, GCP3, GCP4, GCP5, GCP6, and GFP. Error bars in G and I indicate mean ± SD. ***, $P < 0.001$ (two-tailed *t* test). Tub, tubulin.

sites of the mother centrioles, where the SAS-6 even formed rosette-like rings (Fig. 7 B). More importantly, while only ∼3.5% of cells overexpressing NEDD1 WT and 3% overexpressing S325A mutant exhibited more than two SAS-6–positive dots on the duplicated centrosomes, ∼12.5% of the cells overexpressing NEDD1 S325E possessed more than two SAS-6–positive dots or even two SAS-6–positive rosette-like rings around NEDD1 S325E on the duplicated centrosomes (Fig. 7, B and C). When we overexpressed GFP-SAS-6 in U2OS cells and performed immunofluorescence labeling for PLK4 and STIL, we found that

Downloaded from http://rupress.org/jcb/article-pdf/220/1/e202002151/1621362/jcb_202002151.pdf by guest on 09 February 2026

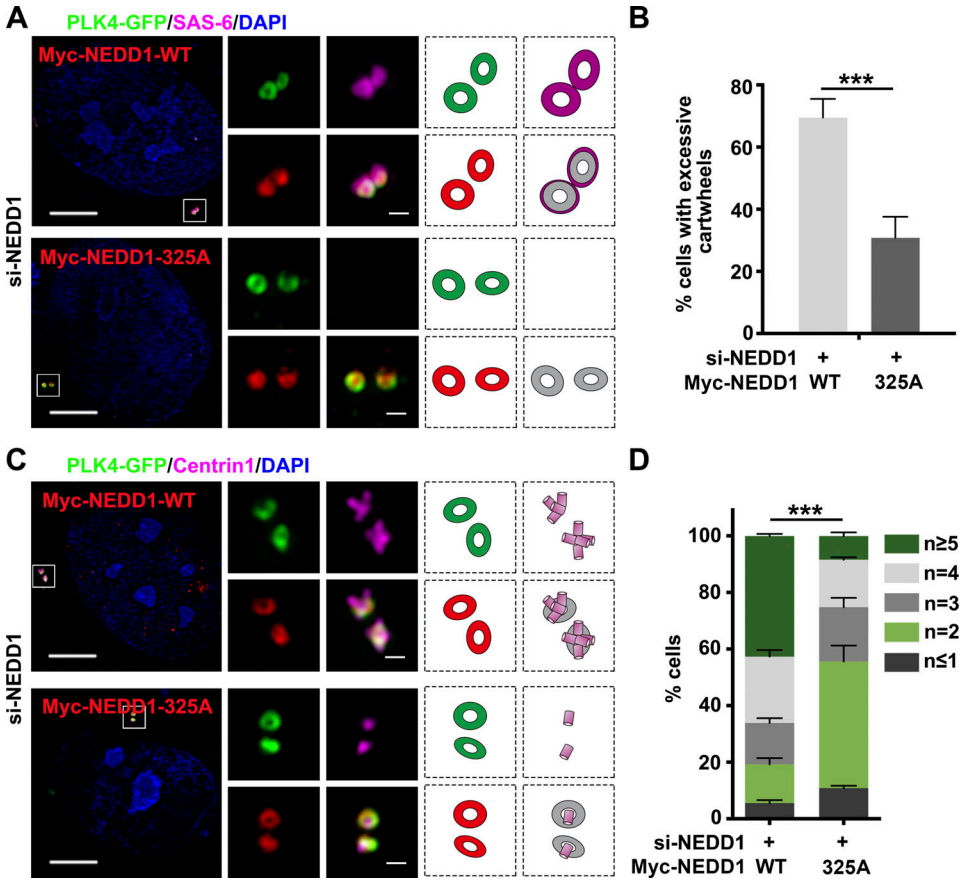

Figure 6. **S325A mutant NEDD1 abolishes centrosome amplification induced by PLK4 overexpression. (A)** U2OS cells were transfected with endogenous NEDD1 siRNA, cotransfected with PLK4-GFP and Myc-tagged siRNA-resistant WT or S325A mutant NEDD1, and coimmunostained with antibodies against Myc and SAS-6. DNA was stained with DAPI. Scale bars, 5 µm (large images) or 0.5 µm (inset images). **(B)** Comparisons of percentages of cells with excessive cartwheels (more than two SAS-6 dots) in A. Three independent replicates of >100 cells per replicate were quantified. **(C)** U2OS cells were transfected with endogenous NEDD1 siRNA, cotransfected with PLK4-GFP and Myc-tagged siRNA-resistant WT or S325A mutant NEDD1, and coimmunostained with antibodies against Myc and Centrin1. DNA was stained with DAPI. Scale bars, 5 µm (large images) or 0.5 µm (inset images). **(D)** Percentages of the cells with different numbers of centrioles and comparisons of those cells with more than four centrioles in each treatment in C. Three independent replicates of >100 cells per replicate were quantified. Error bars in B and D indicate mean ± SD. ***, $P < 0.001$ (two-tailed *t* test).

overexpressed GFP-SAS-6 and endogenous STIL assembled into the rosette-like rings. Interestingly, PLK4 also exhibited a circular localization pattern and was partially colocalized with the outside SAS-6/STIL rosette-like rings (Fig. 7 D). This suggests that the assembly of multiple cartwheels also requires full kinase ability of PLK4 in the circular structure to phosphorylate NEDD1 protein. Consistently, when GFP-tagged NEDD1 WT or mutant proteins were co-overexpressed with Myc-tagged SAS-6 in cells, we found that GFP-tagged NEDD1 S325E recruited much more Myc-SAS-6 than did either the WT or S325A mutant to the PCM, where they formed rosette-like rings to assemble cartwheels (Fig. 7, E and F). By labeling for Centrin1, we further observed that NEDD1 S325E clearly performed multiple daughter centriole biogenesis (Fig. 7, G and H). More strikingly, we found that during mitosis, NEDD1 S325E-overexpressing cells assembled multipolar mitotic spindles and that each pole exhibited NEDD1 S325E and SAS-6 signals, thus suggesting that the poles were structurally normal and functional. However, cells overexpressing NEDD1 WT or S325A assembled only bipolar spindles (Fig.7, I and J). Since NEDD1 S325E mutant overexpression was relatively weaker at driving multiple cartwheels and daughter centrioles than that of PLK4 (Fig. 2, A–E; and Fig. 7, B–H), we suspected that other regulated sites on NEDD1 in addition to S325 may also contribute to cartwheel assembly and daughter centriole biogenesis initiations. Taken together, these results demonstrate that NEDD1, locally phosphorylated by PLK4, recruits SAS-6 to the PCM for cartwheel assembly followed by daughter centriole biogenesis. When excess NEDD1 proteins on the PCM are phosphorylated by PLK4, as observed when PLK4 or the PLK4-phosphorylation–mimicking NEDD1 mutant was overexpressed, those phosphorylated NEDD1 proteins may induce amplification of functional centrosomes by recruiting excess SAS-6 for cartwheel assembly and subsequent daughter centriole biogenesis.

Discussion

The centrosome cycle is highly coupled with the cell cycle and consists of a few main steps. First, the centriole disengages during mitotic exit and early G1 phase, characterized by the loss

Downloaded from http://rupress.org/jcb/article-pdf/220/1/e202002151/1621362/jcb_202002151.pdf by guest on 09 February 2026

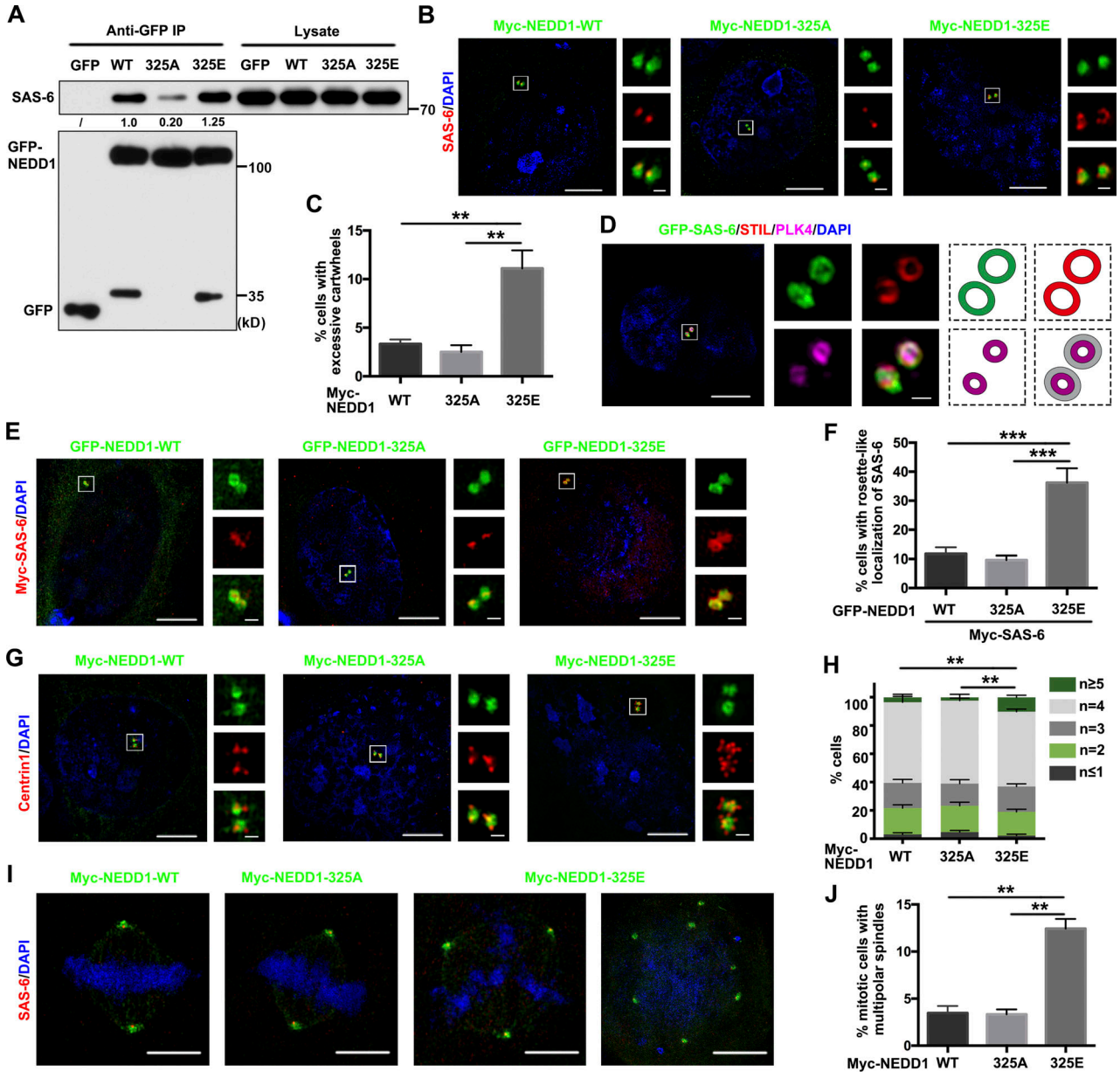

Figure 7. **Phosphomimetic NEDD1 S325E mutant induces centrosome amplification by recruiting excessive SAS-6. (A)** HEK293T cells transfected with GFP-NEDD1 or S325A or S325E mutants and then synchronized at the G1/S transition were released into fresh medium for 4 h. Total cellular extracts were then immunoprecipitated with GFP-Trap beads and probed with antibodies against SAS-6 and GFP. The numbers under the bands refer to the corresponding relative gray value intensity quantified by ImageJ. This experiment was repeated three times, but only one representative result is shown. The intensity of WT group was arbitrarily set as 1.0. **(B)** U2OS cells were transfected with Myc-tagged WT, S325A mutant, or S325E mutant NEDD1 and coimmunostained with anti-SAS-6 antibody. DNA was stained with DAPI. Scale bars, 5 µm (large images) or 0.5 µm (inset images). **(C)** Comparisons of the percentages of cells in B with more than two SAS-6 dots. Three independent replicates of >100 cells per replicate were quantified. **(D)** U2OS cells were transfected with GFP-SAS-6 and immunostained with antibodies against STIL and PLK4. Those proteins' stained features are shown in the cartoons on the right. DNA was stained with DAPI. Scale bars, 5 µm (large images) or 0.5 µm (inset images). **(E)** U2OS cells were cotransfected with GFP-tagged WT or mutant NEDD1 and Myc-SAS-6 and then immunostained with anti-Myc antibody. DNA was stained with DAPI. Scale bars, 5 µm (large images) or 0.5 µm (inset images). **(F)** Comparisons of the percentages of cells with SAS-6 in rosette-like structures in E. Three independent replicates of >100 cells per replicate were quantified. **(G)** U2OS cells were transfected with Myc-tagged WT, S325A mutant, or S325E mutant NEDD1 and immunostained with anti-Centrin1 antibody. DNA was stained with DAPI. Scale bars, 5 µm (large images) or 0.5 µm (inset images). **(H)** Percentages of the cells with different numbers of centrioles and comparisons of those cells with more than four centrioles in each treatment in G. Three independent replicates of >100 cells per replicate were quantified. **(I)** U2OS cells were transfected with Myc-tagged WT, 325A mutant, or 325E mutant NEDD1 and immunostained with anti–SAS-6 antibody. DNA was stained with DAPI. Scale bars, 5 µm (large images) or 0.5 µm (inset images). **(J)** Comparisons of the percentages of cells with multipolar spindles in I. Three independent replicates of >100 cells per replicate were quantified. Error bars in C, F, H, and J indicate mean ± SD. **, P < 0.01; ***, P < 0.001 (two-tailed *t* test).

Downloaded from http://rupress.org/jcb/article-pdf/220/1/e202002151/1621362/jcb_202002151.pdf by guest on 09 February 2026

of the orthogonal arrangement of paired centrioles under the regulation of PLK1, CDK1, and separase (Cabral et al., 2013; Oliveira and Nasmyth, 2013; Tsou et al., 2009). Daughter centriole biogenesis then initiates with the assembly of a cartwheel perpendicular to each preexisting mother centriole during late G1 and S phases (Conduit et al., 2015), and the daughter centrioles elongate through nucleation of centriolar microtubules around the cartwheel by γ-TURC during S and G2 phases, a process under the antagonistic regulations of CPAP and CP110 (Guichard et al., 2010; Kollman et al., 2010; Lin et al., 2013b; Schmidt et al., 2009). The resulting centrosomes subsequently mature and separate to form two matured polar centrosomes destining to regulate mitotic spindle assembly during the G2/M transition (Bahmanyar et al., 2008; Bertran et al., 2011; Faragher and Fry, 2003; Mardin et al., 2011; Mardin et al., 2010; Nam and van Deursen, 2014; Smith et al., 2011). Obviously, cartwheel assembly and subsequent daughter centriole biogenesis are key steps in the centrosome cycle. Increasing evidence indicates that PCM components play crucial roles in controlling the centrosome cycle. However, although extremely important, the underlying mechanisms by which PCM components participate in cartwheel assembly remains poorly understood. In this study, we demonstrate that PLK4-phosphorylated NEDD1 is required for cartwheel assembly initiation, which interacts directly with SAS-6 and recruits it onto the NEDD1-containing layer of the highly ordered, hierarchical PCM.

PLK4, a master regulator of centrosome duplication, phosphorylates several centrosome duplication related proteins and was shown to regulate cartwheel assembly in *Drosophila melanogaster* by phosphorylating Ana2 (STIL in humans), thus triggering SAS-6 recruitment to appropriate sites at the mother centrioles (Dzhindzhev et al., 2014), although this regulation process might not be conserved in other species. In humans, PLK4 phosphorylates STIL to facilitate formation of the STIL–SAS-6 complex (Moyer et al., 2015; Ohta et al., 2014). Intriguingly, STIL could not be detected at the centrioles in the absence of SAS-6, while robust or weak SAS-6 signals were readily detected at the centrioles following depletion of STIL (Arquint et al., 2012; Tang et al., 2011). Therefore, although the PLK4 phosphorylation of STIL apparently contributes to efficient integration of SAS-6 into new daughter centrioles, SAS-6 might be the more important component for initiating cartwheel assembly, and other means also appear to recruit it to the PCM in mammals. Indeed, here, we found that NEDD1 situates upstream of SAS-6 and recruits the latter to the NEDD1-containing layer of the PCM for initiation of cartwheel assembly.

Clearly, cartwheel assembly normally occurs at only one site at the mother centriole, although the PCM organizes into a highly ordered hierarchical structure at the proximal end of each mother centriole under physiological conditions. Under experimental conditions, overexpressed PLK4 forms a persistent ring that overlaps some PCM components, instead of the ring-to-dot-like structure found under physiological conditions. During that experimental condition, cartwheel assembly may be initiated at multiple sites near the proximal end of the mother centriole. This may indicate that to initiate cartwheel assembly, PLK4 regulates a previously unknown key PCM component. In this work, we found that this key PCM component is NEDD1. We revealed that, under physiological conditions, PLK4 colocalizes with NEDD1 at one site at the NEDD1 ring, where cartwheel assembly takes place, and locally phosphorylates NEDD1 at multiple amino acid residues, including S325. The phosphorylation of NEDD1 at S325 enhances the binding of NEDD1 with SAS-6 and recruits the latter to the cartwheel assembly initiation site. Overexpressed PLK4 may phosphorylate more NEDD1 protein in the NEDD1 ring, which in turn recruits more SAS-6 for cartwheel assembly initiation at multiple sites on each mother centriole. Here, we demonstrated that PLK4-phosphorylated NEDD1 indeed binds and recruits SAS-6 to sites at the mother centrioles for cartwheel assembly. By generating a phosphomimicking NEDD1 S325E mutant and overexpressing it in cells, we observed the NEDD1 mutant recruiting more than the usual amount of SAS-6 and thus inducing multiple cartwheel assemblies and subsequent functional daughter centriole biogenesis.

NEDD1 is an evolutionarily conserved protein that was initially identified as a growth suppressor gene in mouse neuroblastoma cells (Kumar et al., 1994). It has been characterized as a potential mediator of γ-TuRC attachment to the mammalian centrosome and is necessary for microtubule nucleation and spindle assembly (Haren et al., 2006; Lüders et al., 2006). Subsequently, NEDD1 was found to be phosphorylated by CDK1, PLK1, Nek9, and Aurora A, targeting γ-TuRC to mitotic spindle microtubules and centrosomes for mitotic spindle assembly (Pinyol et al., 2013; Sdelci et al., 2012; Zhang et al., 2009). Here, we showed that the function of NEDD1 in the initiation of both cartwheel assembly and subsequent daughter centriole biogenesis in interphase cells was under phosphorylation regulation by PLK4 at amino acid residues different from those phosphorylated by other kinases in mitosis. We found that the phosphorylation of NEDD1 at S325 promotes its binding with SAS-6, and this phosphorylation facilitates cartwheel assembly initiation, while subsequent dephosphorylation of NEDD1 at this site may promote its binding with γ-TuRC for daughter centriole biogenesis.

Based on our and others results, we propose a working model to illustrate the functions of PLK4-regulated NEDD1 in the centrosome cycle (Fig. 8). Generally, the PCM hierarchical structure is constructed by a tightly regulated, sequential recruitment of its components dictated by the cell cycle. Cep192 adopts a toroid-like distribution around the mother centriole, while PCNT extends outward toward the periphery. Both of them appear at the top of the PCM hierarchal construct, where they together recruit NEDD1 to form a NEDD1-containing layer that recruits γ-TuRC, so that NEDD1 can colocalize with PLK4 during the G1 phase. Then, PLK4 phosphorylates NEDD1 at S325, thus releasing NEDD1 from interacting with γ-TuRC and allowing it to facilitate cartwheel assembly initiation in early S phase. It does so by directly interacting with and recruiting SAS-6 to the NEDD1-containing layer, where SAS-6 then forms a complex with STIL to assemble the cartwheel. Subsequently, during late S phase to G2 phase, dephosphorylated NEDD1 interacts with γ-TuRC to nucleate centriolar microtubules for daughter centriole biogenesis. Under experimental conditions that cause

Downloaded from http://rupress.org/jcb/article-pdf/220/1/e202002151/1621362/jcb_202002151.pdf by guest on 09 February 2026

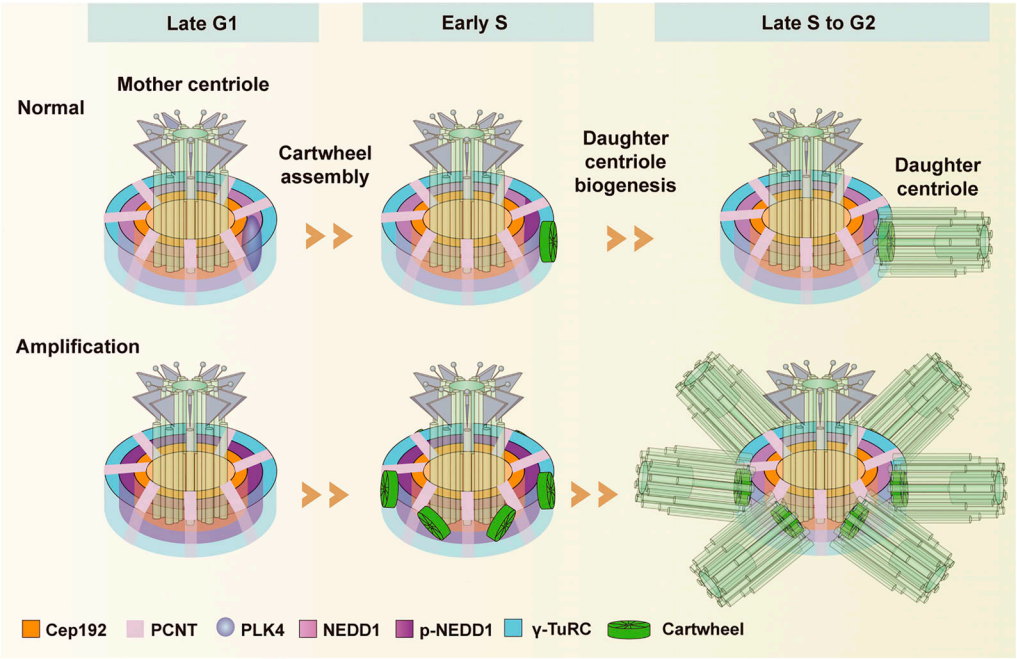

Figure 8. **Model of PLK4-regulated NEDD1 facilitating cartwheel assembly and daughter centriole biogenesis initiations.** Under normal conditions (top progression), in late G1 phase, the mother centriole has PCM component Cep192 adopting a toroid-like distribution, while component PCNT extends outward toward the periphery. Together, the two components recruit NEDD1 to the mother centriole, where it adopts a toroidal distribution and recruits γ-TuRC. Meanwhile, PLK4 is recruited to the site of daughter centriole biogenesis by Cep192 and Cep152, and it colocalizes with NEDD1. Then in early S phase, PLK4 phosphorylates NEDD1 at S325 to switch binding partner preference of NEDD1 from γ-TuRC to SAS-6, recruiting SAS-6 to form a complex with STIL for cartwheel assembly. Subsequently, during S phase and into G2 phase, unphosphorylated NEDD1 increases its interaction with γ-TuRC to nucleate centriolar microtubules for daughter centriole biogenesis. In the bottom progression (amplification), the hyperphosphorylation of NEDD1 can induce centrosome amplification by recruiting excessive SAS-6.

hyperphosphorylation of NEDD1, centrosome amplification may be promoted due to recruitment of excessive SAS-6 to the centrosomes. Our work first shows that NEDD1 facilitates initiation of both cartwheel assembly and subsequent daughter centriole biogenesis by serving as a pedestal, and then clarifies the precise location of cartwheel assembly. These findings provide important information for understanding the underlying mechanisms by which the centrosome cycle is coupled with cell cycle control.

Materials and methods

Plasmids and antibodies

Human *NEDD1* was cloned from a cDNA library by RT-PCR and inserted into pEGFP-C1 (Clontech), pCMV-Myc (Clontech), pQLinkMx-MBP (Maltose Binding Protein; Addgene), and pCAG-Strep (Addgene) vectors. Mutant *NEDD1* constructs were generated by PCR site-directed mutagenesis and then inserted into the pEGFP-C1, pCMV-Myc, and pCAG-Strep vectors. Human *PLK4* was cloned from a cDNA library by PCR and inserted into the pEGFP-N3 (Clontech), pCMV-Myc, and pGEX-4T-1 (Amersham Bioscience) vectors. Human *SAS-6* was cloned from a cDNA library by PCR and inserted into the pEGFP-C1, pCMV-Myc, and pBM-GFP-Strep (Invitrogen) vectors. Human *STIL* was cloned from a cDNA library by PCR and inserted into the pEGFP-C1 and pCMV-Myc vectors. Human *CEP192* was cloned from a cDNA library by PCR and inserted into the p3×FLAG-CMV-7.1 (Sigma-Aldrich) vectors.

Anti-NEDD1 (rabbit and mouse) polyclonal antibodies were raised against the C-terminus (341 end) of human NEDD1 and affinity purified. Anti-PLK4 antibody used for Western blotting (1:500) was generated by immunizing mice with bacterially expressed recombinant PLK4 (amino acids 1–100 at the N-terminus) tagged with GST. The rabbit anti-PLK4 antibody used for immunofluorescence (1:200), was provided by Dr. Monica Bettencourt-Dias (Instituto Gulbenkian de Ciencia, Oeiras, Portugal). For immunofluorescence analysis, we used mouse anti-SAS-6 (sc-81431; Santa Cruz Biotechnology; 1:100), mouse anti-γ-tubulin (T6557; Sigma-Aldrich; 1:200), mouse anti-acetylated α-tubulin (T7451; Sigma-Aldrich; 1:200), and rabbit anti-Centrin 1 (12794–1-AP; Proteintech; 1:200), rabbit anti-STIL (ab89314; Abcam; 1:100), rabbit anti-CDK5RAP2 (ab70213; Abcam, 1:100), rabbit anti-PCNT (ab4448; Abcam; 1:100), rabbit anti-Cep152 (R36074; Abnova; 1:100), and rabbit anti-Cep192 (CSB-PA851560LA01HU; Cusabio; 1:100) antibodies. For Western blotting, we used rabbit anti-STIL (ab89314; Abcam; 1:2,000) and mouse anti-GFP (M048-3; MBL; 1:2,000), mouse anti-Myc (M4439; Sigma-Aldrich; 1:1,000), mouse anti-α-tubulin (T3559; Sigma-Aldrich; 1:1,000), mouse anti-γ-tubulin (T6557; Sigma-Aldrich; 1:1,000), mouse anti-SAS-6 (sc-81431; Santa Cruz Biotechnology; 1:1,000), mouse anti-GCP2 (sc-377117; Santa Cruz Biotechnology; 1:1,000), mouse anti-GCP3 (sc-373758; Santa Cruz Biotechnology; 1:1,000), mouse anti-GCP4 (sc-271876; Santa Cruz Biotechnology; 1:1,000), mouse anti-GCP5 (sc-365837; Santa Cruz Biotechnology; 1:1,000), mouse anti-GCP6 (sc-374063;

Downloaded from http://rupress.org/jcb/article-pdf/220/1/e202002151/1621362/jcb_202002151.pdf by guest on 09 February 2026

Santa Cruz Biotechnology; 1:1,000), and mouse anti-Flag (M185-3L; MBL; 1:2,000) antibodies.

All animal experiments were performed in the Laboratory Animal Center of Peking University and followed the National Institutes of Health Guide for the Care and Use of Laboratory Animals according to guidelines approved by the Institutional Animal Care and Use Committee at Peking University.

Plasmid DNA transfection and RNA interference

Cultured U2OS cells at 40% confluency were transfected with plasmid DNA using TurboFect (Thermo Fisher Scientific). For each 35-mm dish, 2 µg plasmid DNA and 5 µl TurboFect were added to DMEM (final volume, 300 µl), and the mixture was incubated for 20 min. The mixture was then added to U2OS cells with 2 ml medium and incubated for 4 h, and the medium was then replaced with fresh medium. We obtained the following siRNAs from GenePharma: NEDD1 siRNA (5′-GGGCAAAAGCAG ACATGTG-3′), SAS-6 siRNA (5′-UUAACUGUUUGGUAACUGCCC AGGG-3′), STIL siRNA (5′-GTTTAAGGGAAAAGTTATT-3′), Cep192 siRNA (5′-CAGAGGAATCAATAATAAA-3′), PCNT siRNA (5′-UGGACGUCAUCCAAUGAGA-3′), CDK5RAP2 siRNA (5′-UGGAAG AUCUCCUAACUAA-3′), γ-tubulin siRNA (5′-GGAGGACAUGUU CAAGGAATT-3′), and a nontargeting negative control siRNA (5′-UUCUCCGAACGUGUCACGUTT-3′). U2OS cells at 30–40% confluency were transfected with TurboFect following the manufacturer's instructions. For each 35-mm dish, 0.2 mM siRNA and 5 µl TurboFect were added to DMEM (final volume, 300 µl), and the mixture was incubated for 20 min. The mixture was then added to cells with 1.5 ml medium. The medium was replaced with fresh medium after 10 h.

Drug treatment

To examine the recruitment of SAS-6 to centrosomes and centriole numbers, we treated U2OS cells that were arrested in S phase with 2 µg/ml aphidicolin (Sigma-Aldrich) for 24 h. For the HU-induced centriole amplification assay, we grew U2OS cells to 40% confluency on coverslips housed in 35-mm dishes before transfecting them with siRNAs. After transfection for 4 h, we treated the transfected U2OS cells with 16 mM HU (Sigma-Aldrich) for 52 h to arrest the cells in S phase, thus promoting centriole amplification.

To synchronize mitosis, we treated U2OS cells with 2 µg/ml aphidicolin for 24 h and then released them into fresh medium. For double thymidine blockade, we treated HEK293T cells with 2.5 mM thymidine (Sigma-Aldrich) for 18–24 h, released them into fresh medium for 12 h, and blocked again for 18–24 h before releasing them into fresh medium. Both sets of treated cells were held in their respective media until use.

Immunoprecipitation

Approximately 2 mg of the indicated or control antibody was incubated with 25 µl protein A–conjugated Sepharose beads (GE Healthcare, Amersham) in 500 µl of PBS for 1.5 h at 4°C, and the resulting antibody-conjugated protein A beads were washed with immunoprecipitation buffer (20 mM Tris, 150 mM NaCl, 0.5% NP-40, 10 mM NaF, 0.5 mM EGTA, 1 mM Na_3VO_4, and 1 mM PMSF, pH 7.5). The cells were then lysed in immunoprecipitation buffer supplemented with a protease inhibitor cocktail for 15 min at 4°C and then centrifuged at 13,680 *g* for 15 min. We then collected the supernatant and incubated it with antibody- and protein A–conjugated Sepharose beads or 20 µl GFP-Trap beads (Chromo Tek) for 2 h at 4°C. After the beads were washed thoroughly, the proteins were eluted from them and analyzed using SDS-PAGE and Western blotting.

Western blot assays

Protein samples separated by SDS-PAGE were transferred to nitrocellulose membranes, which were then blocked with 3% milk in TTBS (20 mM Tris-HCl, pH 7.4, 500 mM NaCl, and 0.1% Tween 20) for 30 min and incubated with primary antibody overnight at 4°C. After washing three times with TTBS, the membranes were incubated with HRP-conjugated secondary antibody (Jackson ImmunoResearch) diluted 1:5,000 in 3% milk for 1 h at room temperature, and then washed with TTBS. We developed the filters needed for visualization by enhanced chemiluminescence and visualized with x-ray films.

Immunofluorescence

For immunofluorescence assays, we grew cells on coverslips, fixed them in −20°C precooled methanol for 5 min and then incubated them with primary antibodies overnight at 4°C. After washing them three times with PBS, they were incubated with the indicated secondary antibody for 1 h at room temperature. The cells were mounted onto coverslips with Mowiol (Sigma-Aldrich) containing 1 µg/ml DAPI and then examined under an N-SIM superresolution microscope (Nikon).

Superresolution microscopy

We obtained 3D SIM images on an N-SIM imaging system (Nikon) equipped with a 100×/1.49 NA oil-immersion objective (Nikon) and four laser beams (405, 488, 561, and 640 nm), and the highest resolution of the captured images was 120 nm. Laser lines at 405, 488, 561, and 640 nm were used for excitation. Image stacks were acquired at a 0.12 µm interval and computationally reconstructed to generate superresolution optical serial sections with a twofold extended resolution in all four axes. We further processed the reconstructed images for maximum-intensity projections and rendered them in 3D with NIS-Elements AR 4.20.00 (Nikon). The 3D-SIM image resolutions followed a Gaussian distribution with a full width at a half maximum of 130 ± 3 nm.

Protein expression and purification

GST-tagged PLK4 was expressed and purified in PBS from *Escherichia coli* strain BL21 cells. Briefly, we used sonication to lyse the bacterial pellet and then incubated the supernatant with glutathione Sepharose 4B beads (GE Healthcare) at 4°C for 1 h. Nonspecific binding to the resin was eliminated by washing with a threefold resin bed volume of PBS. The purified proteins were eluted with elution buffer (50 mM Tris-HCl, 150 mM NaCl, and 10 mM reduced glutathione, pH 8.0) and dialyzed with PBS.

MBP-tagged NEDD1 was expressed and purified in PBS from *E. coli* strain BL21 cells. Briefly, we used sonication to lyse the bacterial pellet and then incubated the supernatant with Ni Sepharose 6 FF beads (GE Healthcare) at 4°C for 1 h. Nonspecific

Downloaded from http://rupress.org/jcb/article-pdf/220/1/e202002151/1621362/jcb_202002151.pdf by guest on 09 February 2026

binding to the resin was eliminated by washing with a threefold resin bed volume of wash buffer (25 mM Tris-HCl, 150 mM NaCl, and 20 mM imidazole, pH 8.0). The purified proteins were eluted with elution buffer (25 mM Tris-HCl, 150 mM NaCl, and 500 mM imidazole, pH 8.0) and dialyzed with PBS.

Strep-tagged WT and mutant NEDD1 proteins and SAS-6 proteins were expressed and purified from HEK293F cells as follows. The 293F cells were lysed using sonication with extraction buffer (20 mM Tris, 150 mM NaCl, 10 mM NaF, 0.5 mM EGTA, 1 mM Na_3VO_4, and 1 mM PMSF, pH 7.5), and then the supernatant was incubated with Strep-Tactin Sepharose at 4°C for 1 h. Nonspecific binding to the Sepharose was eliminated by washing three times with washing buffer (20 mM Tris and 150 mM NaCl, pH 7.5), and the purified proteins were eluted with elution buffer (20 mM Tris, 150 mM NaCl, and 10 mM desthiobiotin, pH 7.5) and dialyzed against PBS.

In vitro protein interaction assay

We incubated Strep- or MBP-tagged NEDD1 proteins with purified GST, GST-PLK4, GFP-Strep, or GFP-SAS-6-Strep and glutathione Sepharose 4B beads or GFP-Trap beads in immunoprecipitation buffer at 4°C for 3 h.

In vitro kinase activity assay

For the in vitro kinase activity assay, 3 µg samples of WT or mutant NEDD1 proteins were mixed with 1 µg GST-tagged PLK4 in kinase buffer (20 mM Tris-HCl, 10 mM $MgCl_2$, 2 mM KCl, 1 mM DTT, 5 µM Na_3VO_4, 200 mM ATP, and 10 µCi [γ-^{32}P]-ATP, pH 7.5) and incubated at 30°C for 30 min. The samples were then resolved using SDS-PAGE, and the gels were exposed to Kodak film.

Sample preparation for MS analysis

First, Strep-NEDD1 was purified from HEK293F cells and incubated with related proteins and then electrophoresed by SDS-PAGE. The gel was then stained with Coomassie Brilliant Blue to visualize the protein bands, which then underwent tryptic digestion and were subsequently analyzed on an Orbitrap Elite mass spectrometer (Thermo Fisher Scientific) to identify interacting proteins or protein modifications.

Quantification and statistical analysis

The intensity of fluorescent signals was measured using Velocity software (version 6.1.1), and the intensity of immunoblot bands was measured using ImageJ software (version 1.52a; National Institutes of Health). For each statistical graph, three independent replicates were quantified. For fluorescence intensity statistical graphs, three means were used to calculate the average (horizontal bar), standard error of the mean (error bars), and P value. We used Prism software (version 8.0; GraphPad) for statistical analyses using two-tailed *t* tests. Data distribution was assumed to be normal, but this was not formally tested. P values in all graphs were generated with tests as indicated in figure legends and are represented as follows: ns, $P > 0.05$; **, $P < 0.01$; and ***, $P < 0.001$.

Online supplemental material

Fig. S1 includes 3D-SIM images showing that knockdown of NEDD1, but not of γ-tubulin or CDK5RAP2, impairs the localization of cartwheel protein STIL to highlight that NEDD1 is the pedestal for cartwheel formation on the PCM. Fig. S2 shows 3D-SIM images of U2OS cells immunostained with NEDD1 after knocking down Cep192 or PCNT, highlighting the joint recruitment by Cep192 and PCNT of NEDD1 to the PCM. Fig. S3 includes 3D-SIM images showing that centriolar microtubule assembly requires both NEDD1 and γ-tubulin. Fig. S4 3D-SIM images and Western blots show that NEDD1 interacts with SAS-6 and PLK4. The MS data and Western blots in Fig. S5 show that PLK4 phosphorylates NEDD1 and regulates its function.

Acknowledgments

We thank the National Center for Protein Sciences at Peking University (Beijing, China) for assistance with 3D-SIM microscopy and Dr. C.Y. Shan for help with taking SIM images. We also thank Dr. D. Liu for assistance with MS, Dr. H.X. Lv for assistance with using Velocity, and M. Du for drawing the model.

This work was supported by grants from the National Natural Science Foundation of China and the Ministry of Science and Technology of China (2016YFA0500201, 2016YFA0100501, 91854204, 32070714, and 31520103906).

The authors declare no competing financial interests.

Author contributions: C.M. Zhang conceived the project. W.F. Chi, G. Wang, and G.W. Xin designed and performed the experiments. C.M. Zhang, W.F. Chi, and Q. Jiang analyzed the data and wrote the manuscript.

Submitted: 26 February 2020
Revised: 11 September 2020
Accepted: 23 October 2020

References

Arquint, C., K.F. Sonnen, Y.D. Stierhof, and E.A. Nigg. 2012. Cell-cycle-regulated expression of STIL controls centriole number in human cells. *J. Cell Sci.* 125:1342–1352. https://doi.org/10.1242/jcs.099887

Aydogan, M.G., A. Wainman, S. Saurya, T.L. Steinacker, A. Caballe, Z.A. Novak, J. Baumbach, N. Muschalik, and J.W. Raff. 2018. A homeostatic clock sets daughter centriole size in flies. *J. Cell Biol.* 217:1233–1248. https://doi.org/10.1083/jcb.201801014

Aydogan, M.G., T.L. Steinacker, M. Mofatteh, Z.M. Wilmott, F.Y. Zhou, L. Gartenmann, A. Wainman, S. Saurya, Z.A. Novak, S.S. Wong, et al. 2020. An Autonomous Oscillation Times and Executes Centriole Biogenesis. *Cell.* 181:1566–1581.e27. https://doi.org/10.1016/j.cell.2020.05.018

Bahmanyar, S., D.D. Kaplan, J.G. Deluca, T.H. Giddings Jr., E.T. O'Toole, M. Winey, E.D. Salmon, P.J. Casey, W.J. Nelson, and A.I.M. Barth. 2008. beta-Catenin is a Nek2 substrate involved in centrosome separation. *Genes Dev.* 22:91–105. https://doi.org/10.1101/gad.1596308

Bahtz, R., J. Seidler, M. Arnold, U. Haselmann-Weiss, C. Antony, W.D. Lehmann, and I. Hoffmann. 2012. GCP6 is a substrate of Plk4 and required for centriole duplication. *J. Cell Sci.* 125:486–496. https://doi.org/10.1242/jcs.093930

Bertran, M.T., S. Sdelci, L. Regué, J. Avruch, C. Caelles, and J. Roig. 2011. Nek9 is a Plk1-activated kinase that controls early centrosome separation through Nek6/7 and Eg5. *EMBO J.* 30:2634–2647. https://doi.org/10.1038/emboj.2011.179

Bornens, M. 2012. The centrosome in cells and organisms. *Science.* 335:422–426. https://doi.org/10.1126/science.1209037

Cabral, G., S.S. Sans, C.R. Cowan, and A. Dammermann. 2013. Multiple mechanisms contribute to centriole separation in C. elegans. *Curr. Biol.* 23:1380–1387. https://doi.org/10.1016/j.cub.2013.06.043

Downloaded from http://rupress.org/jcb/article-pdf/220/1/e202002151/1621362/jcb_202002151.pdf by guest on 09 February 2026

Conduit, P.T., A. Wainman, and J.W. Raff. 2015. Centrosome function and assembly in animal cells. *Nat. Rev. Mol. Cell Biol.* 16:611–624. https://doi.org/10.1038/nrm4062

Dammermann, A., T. Müller-Reichert, L. Pelletier, B. Habermann, A. Desai, and K. Oegema. 2004. Centriole assembly requires both centriolar and pericentriolar material proteins. *Dev. Cell.* 7:815–829. https://doi.org/10.1016/j.devcel.2004.10.015

Dzhindzhev, N.S., G. Tzolovsky, Z. Lipinszki, S. Schneider, R. Lattao, J. Fu, J. Debski, M. Dadlez, and D.M. Glover. 2014. Plk4 phosphorylates Ana2 to trigger Sas6 recruitment and procentriole formation. *Curr. Biol.* 24:2526–2532. https://doi.org/10.1016/j.cub.2014.08.061

Faragher, A.J., and A.M. Fry. 2003. Nek2A kinase stimulates centrosome disjunction and is required for formation of bipolar mitotic spindles. *Mol. Biol. Cell.* 14:2876–2889. https://doi.org/10.1091/mbc.e03-02-0108

Fu, J.Y., and C.M. Zhang. 2019. Super-resolution microscopy: successful applications in centrosome study and beyond. *Biophys. Rep.* 5:235–243. https://doi.org/10.1007/s41048-019-00101-x

Gomez-Ferreria, M.A., U. Rath, D.W. Buster, S.K. Chanda, J.S. Caldwell, D.R. Rines, and D.J. Sharp. 2007. Human Cep192 is required for mitotic centrosome and spindle assembly. *Curr. Biol.* 17:1960–1966. https://doi.org/10.1016/j.cub.2007.10.019

Guichard, P., D. Chrétien, S. Marco, and A.M. Tassin. 2010. Procentriole assembly revealed by cryo-electron tomography. *EMBO J.* 29:1565–1572. https://doi.org/10.1038/emboj.2010.45

Haren, L., M.H. Remy, I. Bazin, I. Callebaut, M. Wright, and A. Merdes. 2006. NEDD1-dependent recruitment of the gamma-tubulin ring complex to the centrosome is necessary for centriole duplication and spindle assembly. *J. Cell Biol.* 172:505–515. https://doi.org/10.1083/jcb.200510028

Ito, D., S. Zitouni, S.C. Jana, P. Duarte, J. Surkont, Z. Carvalho-Santos, J.B. Pereira-Leal, M.G. Ferreira, and M. Bettencourt-Dias. 2019. Pericentrin-mediated SAS-6 recruitment promotes centriole assembly. *eLife.* 8:e41418. https://doi.org/10.7554/eLife.41418

Joukov, V., J.C. Walter, and A. De Nicolo. 2014. The Cep192-organized aurora A-Plk1 cascade is essential for centrosome cycle and bipolar spindle assembly. *Mol. Cell.* 55:578–591. https://doi.org/10.1016/j.molcel.2014.06.016

Keller, D., M. Orpinell, N. Olivier, M. Wachsmuth, R. Mahen, R. Wyss, V. Hachet, J. Ellenberg, S. Manley, and P. Gönczy. 2014. Mechanisms of HsSAS-6 assembly promoting centriole formation in human cells. *J. Cell Biol.* 204:697–712. https://doi.org/10.1083/jcb.201307049

Kim, T.S., J.E. Park, A. Shukla, S. Choi, R.N. Murugan, J.H. Lee, M. Ahn, K. Rhee, J.K. Bang, B.Y. Kim, et al. 2013. Hierarchical recruitment of Plk4 and regulation of centriole biogenesis by two centrosomal scaffolds, Cep192 and Cep152. *Proc. Natl. Acad. Sci. USA.* 110:E4849–E4857. https://doi.org/10.1073/pnas.1319656110

Kitagawa, D., I. Vakonakis, N. Olieric, M. Hilbert, D. Keller, V. Olieric, M. Bortfeld, M.C. Erat, I. Flückiger, P. Gönczy, and M.O. Steinmetz. 2011. Structural basis of the 9-fold symmetry of centrioles. *Cell.* 144:364–375. https://doi.org/10.1016/j.cell.2011.01.008

Kleylein-Sohn, J., J. Westendorf, M. Le Clech, R. Habedanck, Y.D. Stierhof, and E.A. Nigg. 2007. Plk4-induced centriole biogenesis in human cells. *Dev. Cell.* 13:190–202. https://doi.org/10.1016/j.devcel.2007.07.002

Kollman, J.M., J.K. Polka, A. Zelter, T.N. Davis, and D.A. Agard. 2010. Microtubule nucleating gamma-TuSC assembles structures with 13-fold microtubule-like symmetry. *Nature.* 466:879–882. https://doi.org/10.1038/nature09207

Kumar, S., T. Matsuzaki, Y. Yoshida, and M. Noda. 1994. Molecular cloning and biological activity of a novel developmentally regulated gene encoding a protein with beta-transducin-like structure. *J. Biol. Chem.* 269:11318–11326.

Lawo, S., M. Hasegan, G.D. Gupta, and L. Pelletier. 2012. Subdiffraction imaging of centrosomes reveals higher-order organizational features of pericentriolar material. *Nat. Cell Biol.* 14:1148–1158. https://doi.org/10.1038/ncb2591

Lee, K., and K. Rhee. 2011. PLK1 phosphorylation of pericentrin initiates centrosome maturation at the onset of mitosis. *J. Cell Biol.* 195:1093–1101. https://doi.org/10.1083/jcb.201106093

Lee, M., M.Y. Seo, J. Chang, D.S. Hwang, and K. Rhee. 2017. PLK4 phosphorylation of CP110 is required for efficient centriole assembly. *Cell Cycle.* 16:1225–1234. https://doi.org/10.1080/15384101.2017.1325555

Lin, Y.C., C.W. Chang, W.B. Hsu, C.J.C. Tang, Y.N. Lin, E.J. Chou, C.T. Wu, and T.K. Tang. 2013a. Human microcephaly protein CEP135 binds to hSAS-6 and CPAP, and is required for centriole assembly. *EMBO J.* 32:1141–1154. https://doi.org/10.1038/emboj.2013.56

Lin, Y.N., C.T. Wu, Y.C. Lin, W.B. Hsu, C.J.C. Tang, C.W. Chang, and T.K. Tang. 2013b. CEP120 interacts with CPAP and positively regulates centriole elongation. *J. Cell Biol.* 202:211–219. https://doi.org/10.1083/jcb.201212060

Lüders, J. 2012. The amorphous pericentriolar cloud takes shape. *Nat. Cell Biol.* 14:1126–1128. https://doi.org/10.1038/ncb2617

Lüders, J., U.K. Patel, and T. Stearns. 2006. GCP-WD is a gamma-tubulin targeting factor required for centrosomal and chromatin-mediated microtubule nucleation. *Nat. Cell Biol.* 8:137–147. https://doi.org/10.1038/ncb1349

Lukinavičius, G., D. Lavogina, M. Orpinell, K. Umezawa, L. Reymond, N. Garin, P. Gönczy, and K. Johnsson. 2013. Selective chemical crosslinking reveals a Cep57-Cep63-Cep152 centrosomal complex. *Curr. Biol.* 23:265–270. https://doi.org/10.1016/j.cub.2012.12.030

Mardin, B.R., C. Lange, J.E. Baxter, T. Hardy, S.R. Scholz, A.M. Fry, and E. Schiebel. 2010. Components of the Hippo pathway cooperate with Nek2 kinase to regulate centrosome disjunction. *Nat. Cell Biol.* 12:1166–1176. https://doi.org/10.1038/ncb2120

Mardin, B.R., F.G. Agircan, C. Lange, and E. Schiebel. 2011. Plk1 controls the Nek2A-PP1γ antagonism in centrosome disjunction. *Curr. Biol.* 21:1145–1151. https://doi.org/10.1016/j.cub.2011.05.047

Mennella, V., B. Keszthelyi, K.L. McDonald, B. Chhun, F. Kan, G.C. Rogers, B. Huang, and D.A. Agard. 2012. Subdiffraction-resolution fluorescence microscopy reveals a domain of the centrosome critical for pericentriolar material organization. *Nat. Cell Biol.* 14:1159–1168. https://doi.org/10.1038/ncb2597

Moyer, T.C., K.M. Clutario, B.G. Lambrus, V. Daggubati, and A.J. Holland. 2015. Binding of STIL to Plk4 activates kinase activity to promote centriole assembly. *J. Cell Biol.* 209:863–878. https://doi.org/10.1083/jcb.201502088

Nam, H.J., and J.M. van Deursen. 2014. Erratum: Corrigendum: Cyclin B2 and p53 control proper timing of centrosome separation. *Nat. Cell Biol.* 16:1027. https://doi.org/10.1038/ncb3049

Nigg, E.A., and A.J. Holland. 2018. Once and only once: mechanisms of centriole duplication and their deregulation in disease. *Nat. Rev. Mol. Cell Biol.* 19:297–312. https://doi.org/10.1038/nrm.2017.127

Nigg, E.A., and J.W. Raff. 2009. Centrioles, centrosomes, and cilia in health and disease. *Cell.* 139:663–678. https://doi.org/10.1016/j.cell.2009.10.036

Novak, Z.A., A. Wainman, L. Gartenmann, and J.W. Raff. 2016. Cdk1 Phosphorylates Drosophila Sas-4 to Recruit Polo to Daughter Centrioles and Convert Them to Centrosomes. *Dev. Cell.* 37:545–557. https://doi.org/10.1016/j.devcel.2016.05.022

Ohta, M., T. Ashikawa, Y. Nozaki, H. Kozuka-Hata, H. Goto, M. Inagaki, M. Oyama, and D. Kitagawa. 2014. Direct interaction of Plk4 with STIL ensures formation of a single procentriole per parental centriole. *Nat. Commun.* 5:5267. https://doi.org/10.1038/ncomms6267

Oliveira, R.A., and K. Nasmyth. 2013. Cohesin cleavage is insufficient for centriole disengagement in Drosophila. *Curr. Biol.* 23:R601–R603. https://doi.org/10.1016/j.cub.2013.04.003

Pinyol, R., J. Scrofani, and I. Vernos. 2013. The role of NEDD1 phosphorylation by Aurora A in chromosomal microtubule nucleation and spindle function. *Curr. Biol.* 23:143–149. https://doi.org/10.1016/j.cub.2012.11.046

Puklowski, A., Y. Homsi, D. Keller, M. May, S. Chauhan, U. Kossatz, V. Grünwald, S. Kubicka, A. Pich, M.P. Manns, et al. 2011. The SCF-FBXW5 E3-ubiquitin ligase is regulated by PLK4 and targets HsSAS-6 to control centrosome duplication. *Nat. Cell Biol.* 13:1004–1009. https://doi.org/10.1038/ncb2282

Ramani, A., A. Mariappan, M. Gottardo, S. Mandad, H. Urlaub, T. Avidor-Reiss, M. Riparbelli, G. Callaini, A. Debec, R. Feederle, and J. Gopalakrishnan. 2018. Plk1/Polo Phosphorylates Sas-4 at the Onset of Mitosis for an Efficient Recruitment of Pericentriolar Material to Centrosomes. *Cell Rep.* 25:3618–3630.e6. https://doi.org/10.1016/j.celrep.2018.11.102

Schmidt, T.I., J. Kleylein-Sohn, J. Westendorf, M. Le Clech, S.B. Lavoie, Y.D. Stierhof, and E.A. Nigg. 2009. Control of centriole length by CPAP and CP110. *Curr. Biol.* 19:1005–1011. https://doi.org/10.1016/j.cub.2009.05.016

Sdelci, S., M. Schütz, R. Pinyol, M.T. Bertran, L. Regué, C. Caelles, I. Vernos, and J. Roig. 2012. Nek9 phosphorylation of NEDD1/GCP-WD contributes to Plk1 control of γ-tubulin recruitment to the mitotic centrosome. *Curr. Biol.* 22:1516–1523. https://doi.org/10.1016/j.cub.2012.06.027

Smith, E., N. Hégarat, C. Vesely, I. Roseboom, C. Larch, H. Streicher, K. Straatman, H. Flynn, M. Skehel, T. Hirota, et al. 2011. Differential control of Eg5-dependent centrosome separation by Plk1 and Cdk1. *EMBO J.* 30:2233–2245. https://doi.org/10.1038/emboj.2011.120

Downloaded from http://rupress.org/jcb/article-pdf/220/1/e202002151/1621362/jcb_202002151.pdf by guest on 09 February 2026

Sonnen, K.F., A.M. Gabryjonczyk, E. Anselm, Y.D. Stierhof, and E.A. Nigg. 2013. Human Cep192 and Cep152 cooperate in Plk4 recruitment and centriole duplication. *J. Cell Sci.* 126:3223–3233. https://doi.org/10.1242/jcs.129502

Tang, C.J.C., S.Y. Lin, W.B. Hsu, Y.N. Lin, C.T. Wu, Y.C. Lin, C.W. Chang, K.S. Wu, and T.K. Tang. 2011. The human microcephaly protein STIL interacts with CPAP and is required for procentriole formation. *EMBO J.* 30:4790–4804. https://doi.org/10.1038/emboj.2011.378

Tsou, M.F.B., W.J. Wang, K.A. George, K. Uryu, T. Stearns, and P.V. Jallepalli. 2009. Polo kinase and separase regulate the mitotic licensing of centriole duplication in human cells. *Dev. Cell.* 17:344–354. https://doi.org/10.1016/j.devcel.2009.07.015

van Breugel, M., M. Hirono, A. Andreeva, H.A. Yanagisawa, S. Yamaguchi, Y. Nakazawa, N. Morgner, M. Petrovich, I.O. Ebong, C.V. Robinson, et al. 2011. Structures of SAS-6 suggest its organization in centrioles. *Science.* 331:1196–1199. https://doi.org/10.1126/science.1199325

Wang, G., Q. Jiang, and C. Zhang. 2014. The role of mitotic kinases in coupling the centrosome cycle with the assembly of the mitotic spindle. *J. Cell Sci.* 127:4111–4122. https://doi.org/10.1242/jcs.151753

Xu, X., S. Huang, B. Zhang, F. Huang, W. Chi, J. Fu, G. Wang, S. Li, Q. Jiang, and C. Zhang. 2017. DNA replication licensing factor Cdc6 and Plk4 kinase antagonistically regulate centrosome duplication via Sas-6. *Nat. Commun.* 8:15164. https://doi.org/10.1038/ncomms15164

Zhang, X., Q. Chen, J. Feng, J. Hou, F. Yang, J. Liu, Q. Jiang, and C. Zhang. 2009. Sequential phosphorylation of Nedd1 by Cdk1 and Plk1 is required for targeting of the gammaTuRC to the centrosome. *J. Cell Sci.* 122: 2240–2251. https://doi.org/10.1242/jcs.042747

Zhu, F., S. Lawo, A. Bird, D. Pinchev, A. Ralph, C. Richter, T. Müller-Reichert, R. Kittler, A.A. Hyman, and L. Pelletier. 2008. The mammalian SPD-2 ortholog Cep192 regulates centrosome biogenesis. *Curr. Biol.* 18: 136–141. https://doi.org/10.1016/j.cub.2007.12.055

Downloaded from http://rupress.org/jcb/article-pdf/220/1/e202002151/1621362/jcb_202002151.pdf by guest on 09 February 2026

Supplemental material

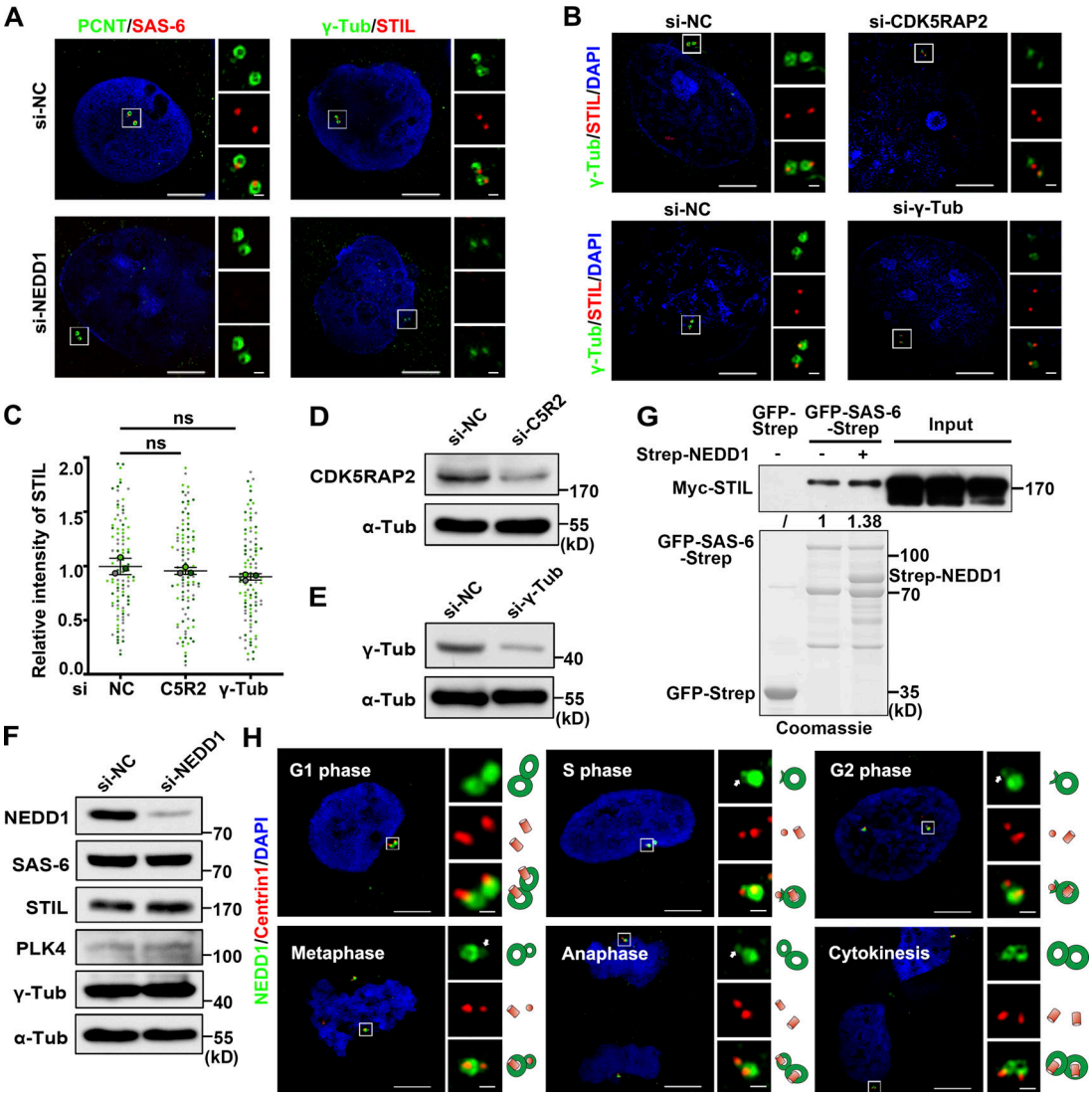

Figure S1. **NEDD1 is the pedestal for cartwheel formation on the PCM. (A)** U2OS cells treated with siRNA against negative control or NEDD1 were coimmunostained with antibodies against γ-tubulin and STIL or PCNT and SAS-6. DNA was stained with DAPI. Scale bars, 5 µm (large images) or 0.5 µm (inset images). **(B)** U2OS cells treated with control, CDK5RAP2, or γ-tubulin siRNA were coimmunostained with antibodies against γ-tubulin and STIL. DNA was stained with DAPI. Scale bars, 5 µm (large images) or 0.5 µm (inset images). **(C)** Comparisons of the relative fluorescence intensity of STIL in B. Three independent replicates of >30 cells per replicate were quantified. ns, no significant difference (two-tailed *t* test). **(D and E)** The efficiency of siRNA-mediated CDK5RAP2 and γ-tubulin depletion in U2OS cells was shown in Western blots with antibodies against CDK5RAP2, γ-tubulin, and α-tubulin. **(F)** HEK293T cells were transfected with control or NEDD1 siRNA. Total cell extracts were probed with antibodies against NEDD1, SAS-6, STIL, PLK4, γ-tubulin, and α-tubulin. **(G)** GFP-Trap beads coupled with purified GFP-Strep or GFP-SAS-6-Strep were incubated with total extracts of HEK293T cells expressing Myc-STIL, either purified Strep-NEDD1 or neither and analyzed using anti-Myc antibody. The indicated protein loads are shown by Coomassie blue staining. The numbers under the bands refer to the corresponding relative gray value intensity quantified by ImageJ. This experiment was repeated three times, but only one representative result is shown. The intensity of the experimental group without Strep-NEDD1 was arbitrarily set as 1.0. **(H)** Immunofluorescence analysis of NEDD1 and Centrin1 in U2OS cells showed that NEDD1 extends toward the daughter centriole as the cell cycle progresses. Arrows denote NEDD1 localization in the daughter centriole. DNA was stained with DAPI. The stained proteins' features are shown in the cartoons on the right. Scale bars, 5 µm (large images) or 0.5 µm (inset images). NC, negative control; Tub, tubulin.

Downloaded from http://rupress.org/jcb/article-pdf/220/1/e202002151/1621362/jcb_202002151.pdf by guest on 09 February 2026

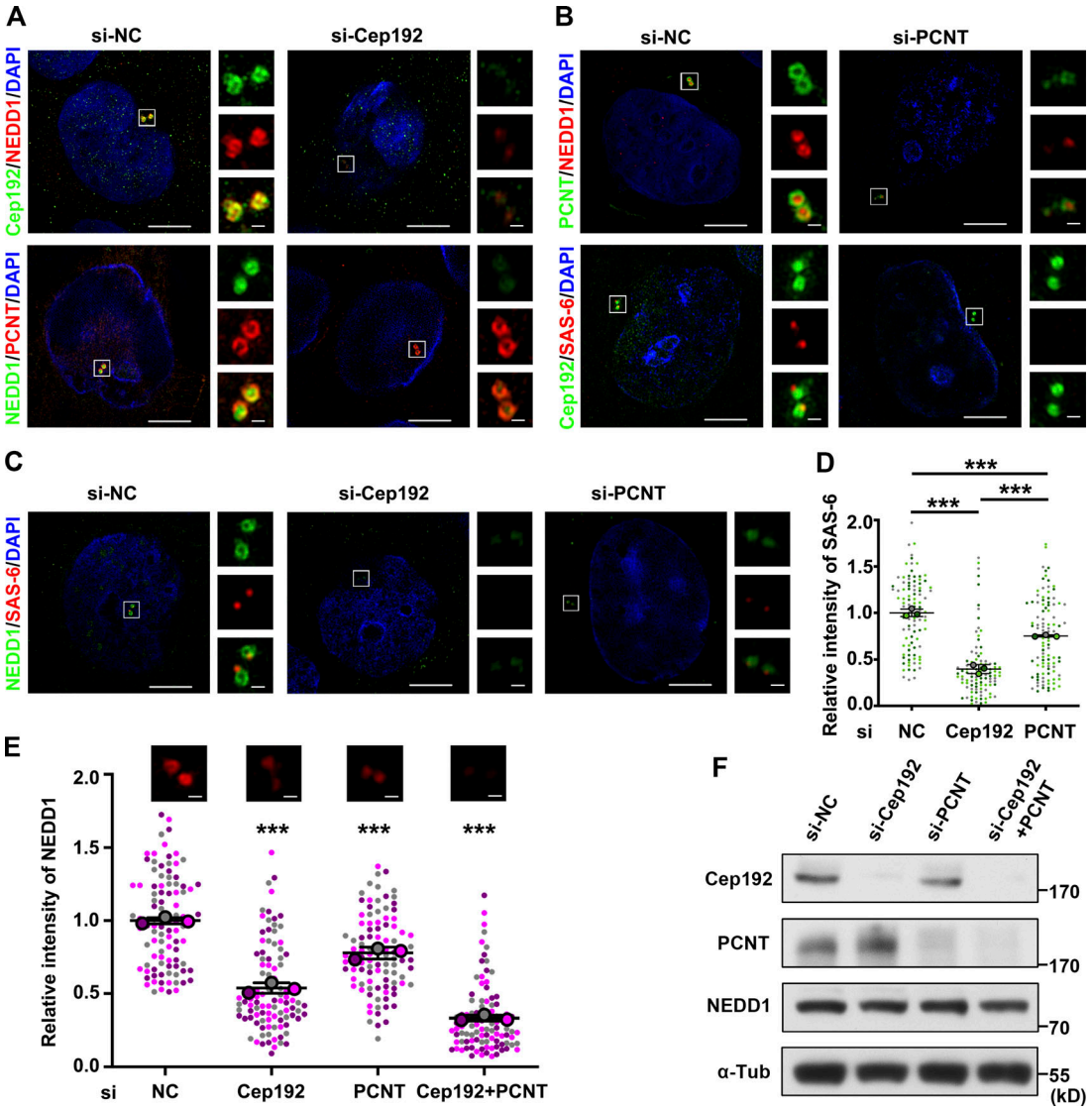

Figure S2. **Cep192 and PCNT together recruit NEDD1 to the PCM. (A)** U2OS cells treated with negative control or Cep192 siRNA were coimmunostained with antibodies against Cep192 and NEDD1 or against NEDD1 and PCNT. DNA was stained with DAPI. Scale bars, 5 µm (large images) or 0.5 µm (inset images). **(B)** U2OS cells treated with control or PCNT siRNA were coimmunostained with anti-PCNT and anti-NEDD1 or with anti-Cep192 and anti-SAS-6 antibodies. DNA was stained with DAPI. Scale bars, 5 µm (large images) or 0.5 µm (inset images). **(C)** U2OS cells treated with control, Cep192, or PCNT siRNA were coimmunostained with antibodies against NEDD1 and SAS-6. DNA was stained with DAPI. Scale bars, 5 µm (large images) or 0.5 µm (inset images). **(D)** Comparisons of the SAS-6 relative fluorescence intensity in C. Three independent replicates of >30 cells per replicate were quantified. Error bars indicate mean ± SD. ***, $P < 0.001$ (two-tailed *t* test). **(E)** Comparisons of the NEDD1 relative fluorescence intensities on centrosomes. Scale bars, 0.5 µm. Three independent replicates of >30 cells per replicate were quantified. Error bars indicate mean ± SD. ***, $P < 0.001$ (two-tailed *t* test). **(F)** Efficiencies of siRNA-mediated Cep192 and PCNT depletions in U2OS cells as shown in Western blots with antibodies against Cep192, PCNT, NEDD1, and α-tubulin. NC, negative control; Tub, tubulin.

Downloaded from http://rupress.org/jcb/article-pdf/220/1/e202002151/1621362/jcb_202002151.pdf by guest on 09 February 2026

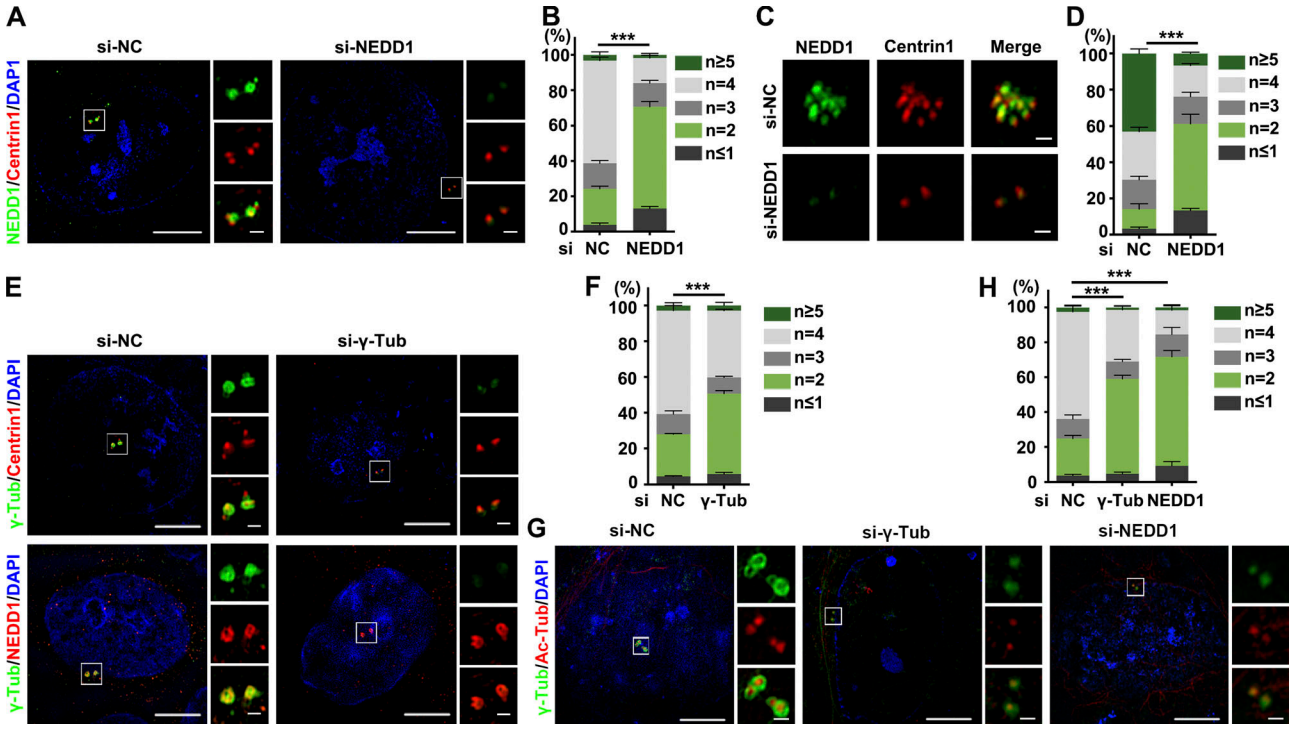

Figure S3. **Both NEDD1 and γ-tubulin are necessary for centrosome duplication. (A)** U2OS cells treated with negative control or NEDD1 siRNA were coimmunostained with antibodies against NEDD1 and Centrin1. DNA was stained with DAPI. Scale bars, 5 µm (large images) or 0.5 µm (inset images). **(B)** Percentages of the cells with different numbers of centrioles and comparisons of those cells with fewer than four centrioles in each treatment in A. Three independent replicates of >100 cells per replicate were quantified. **(C)** U2OS cells transfected with the corresponding siRNA and treated with 16 mM HU to allow centriole amplification were then stained with antibodies against NEDD1 and Centrin1. DNA was stained with DAPI. Scale bars, 0.5 µm. **(D)** Percentages of the cells with different numbers of centrioles and comparisons of those cells with >4 centrioles in each treatment in (C). Three independent replicates of >100 cells per replicate were quantified. **(E)** U2OS cells treated with control or γ-tubulin siRNA were coimmunostained with antibodies against γ-tubulin and Centrin1 or γ-tubulin and NEDD1. DNA was stained with DAPI. Scale bars, 5 µm (large images) or 0.5 µm (inset images). **(F)** Percentages of the cells with different numbers of centrioles and comparisons of those cells with fewer than four centrioles in each treatment in E. Three independent replicates of >100 cells per replicate were quantified. **(G)** U2OS cells treated with control, γ-tubulin, or NEDD1 siRNA were coimmunostained with antibodies against γ-tubulin and acetylated tubulin. DNA was stained with DAPI. Scale bars, 5 µm (large images) or 0.5 µm (inset images). **(H)** Percentages of the cells with different numbers of centrioles and comparisons of those cells with fewer than four acetylated-tubulin dots in each treatment in G. Three independent replicates of >100 cells per replicate were quantified. Error bars in B, D, F, and H indicate mean ± SD. ***, $P < 0.001$ (two-tailed *t* test). NC, negative control; Tub, tubulin.

Downloaded from http://rupress.org/jcb/article-pdf/220/1/e202002151/1621362/jcb_202002151.pdf by guest on 09 February 2026

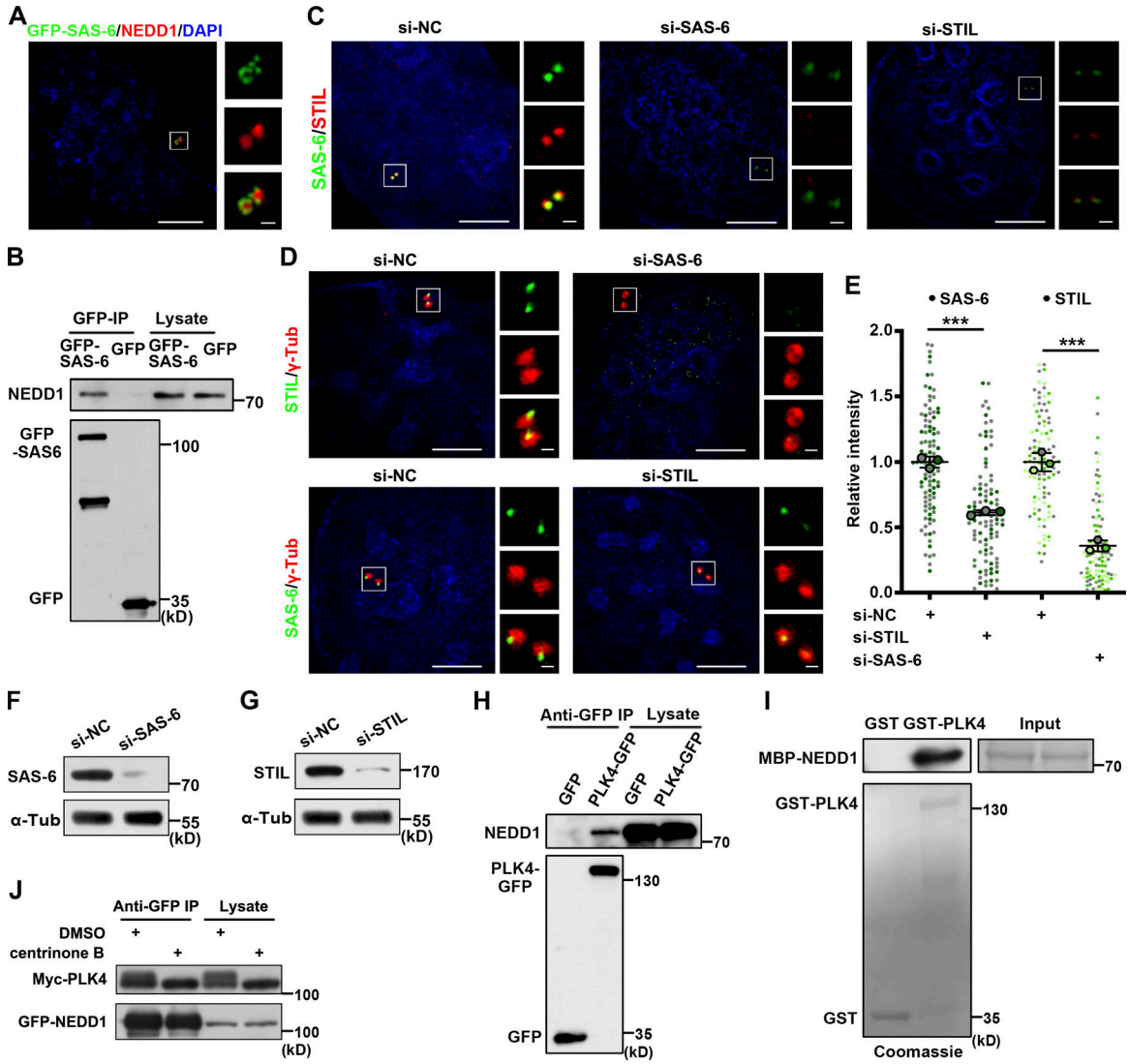

Figure S4. **NEDD1 interacts with SAS-6 and PLK4. (A)** U2OS cells transfected with GFP-SAS-6 were stained with anti-NEDD1 antibody. DNA was stained with DAPI. Scale bars, 5 µm (large images) or 0.5 µm (inset images). **(B)** HEK293T cells were transfected with GFP-SAS-6. Total cell extracts were immunoprecipitated with GFP-Trap beads and probed with antibodies against NEDD1 and GFP. **(C)** U2OS cells treated with siRNA against SAS-6 or STIL were coimmunostained with antibodies against SAS-6 and STIL. DNA was stained with DAPI. Scale bars, 5 µm (large images) or 0.5 µm (inset images). **(D)** U2OS cells treated with siRNA against SAS-6 or STIL were coimmunostained with antibodies against STIL and γ-tubulin or against SAS-6 and γ-tubulin. DNA was stained with DAPI. Scale bars, 5 µm (large images) or 0.5 µm (inset images). **(E)** Comparisons of the relative fluorescence intensities in D. Three independent replicates of >30 cells per replicate were quantified. Error bars indicate mean ± SD. ***, $P < 0.001$ (two-tailed *t* test). **(F and G)** The efficiency of siRNA-mediated SAS-6 and STIL depletion in U2OS cells shown by Western blotting with antibodies against SAS-6, STIL, and α-tubulin. **(H)** HEK293T cells were transfected with PLK4-GFP. Total cell extracts were immunoprecipitated with GFP-Trap beads and probed with antibodies against NEDD1 and GFP. **(I)** In vitro PLK4 and NEDD1 binding assay. Sepharose beads coupled with purified GST or GST-PLK4 were incubated with MBP-NEDD1 purified from *E. coli* and analyzed using anti-NEDD1 antibody. The indicated protein loads are shown by Coomassie blue staining. **(J)** HEK293T cells were cotransfected with GFP-tagged NEDD1 and Myc-tagged PLK4 and treated with DMSO or 500 nM centrinone B for 24 h. Then, total cell extracts were immunoprecipitated with GFP-Trap beads and probed with antibodies against Myc and GFP. NC, negative control; Tub, tubulin.

Downloaded from http://rupress.org/jcb/article-pdf/220/1/e202002151/1621362/jcb_202002151.pdf by guest on 09 February 2026

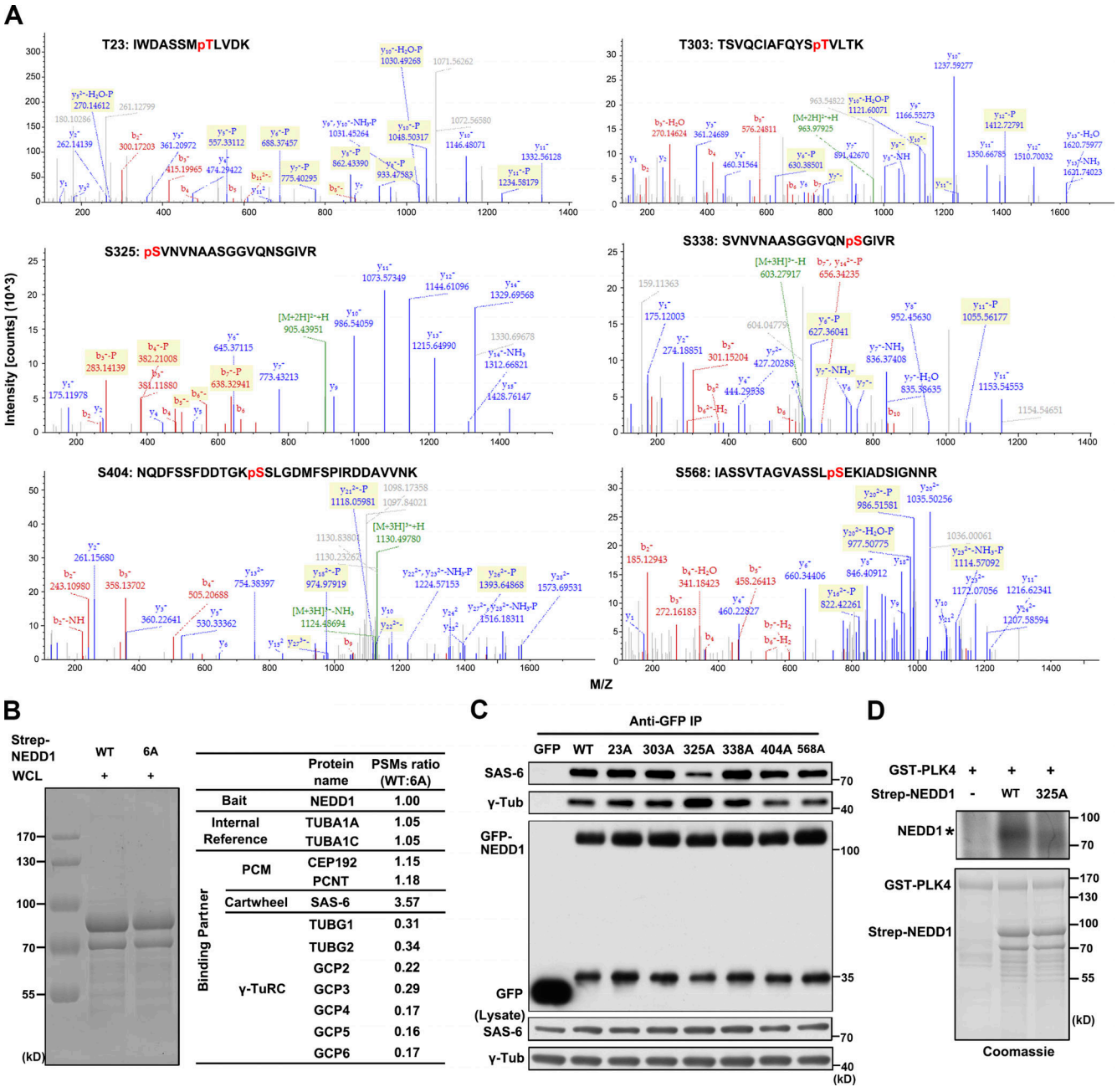

Figure S5. **PLK4 phosphorylates NEDD1 and regulates its function. (A)** MS results of the six sites in NEDD1 that were phosphorylated by PLK4. **(B)** Strep beads coupled with equivalent Strep-tagged WT or 6A mutant NEDD1 purified from HEK293F cells were incubated with HEK293T whole-cell lysates (WCL). With NEDD1 used as bait and TUBA1A/C used as internal references, the interacting proteins were analyzed by MS. The results were quantified as follows: peptide spectrum match (PSM) ratio = PSMs of *X* protein pulled down by WT NEDD1/PSMs of *X* protein pulled down by 6A NEDD1. **(C)** HEK293T cells were transfected with GFP-tagged WT or NEDD1 mutants, and then total cellular extracts were immunoprecipitated with GFP-Trap beads and probed with antibodies against SAS-6, γ-tubulin, and GFP. **(D)** Purified GST-PLK4 was incubated with purified Strep-NEDD1 or S325A mutant NEDD1 proteins in the presence of [γ-^{32}P]-ATP and followed by autoradiography. Coomassie blue was used as a loading stain. *, phosphorylated NEDD1. Tub, tubulin.

Downloaded from http://rupress.org/jcb/article-pdf/220/1/e202002151/1621362/jcb_202002151.pdf by guest on 09 February 2026